

Doctorate Program in Molecular  
Oncology and Endocrinology  
Doctorate School in Molecular  
Medicine

XXIII cycle - 2007–2010  
Coordinator: Prof. Giancarlo Vecchio

**“PED/PEA-15 regulates wound healing and angiogenesis by  
affecting cytoskeletal organization and cell motility: a model  
for diabetic complications”**

Roberta Buonomo

University of Naples Federico II  
Dipartimento di Biologia e Patologia Cellulare e Molecolare  
“L. Califano”

## **Administrative Location**

Dipartimento di Biologia e Patologia Cellulare e Molecolare “L. Califano”  
Università degli Studi di Napoli Federico II

### **Partner Institutions**

#### **Italian Institutions**

Università degli Studi di Napoli “Federico II”, Naples, Italy  
Istituto di Endocrinologia ed Oncologia Sperimentale “G. Salvatore”, CNR, Naples, Italy  
Seconda Università di Napoli, Naples, Italy  
Università degli Studi di Napoli “Parthenope”, Naples, Italy  
Università del Sannio, Benevento, Italy  
Università di Genova, Genoa, Italy  
Università di Padova, Padua, Italy  
Università degli Studi “Magna Graecia”, Catanzaro, Italy  
Università degli Studi di Firenze, Florence, Italy  
Università degli Studi di Bologna, Bologna, Italy  
Università degli Studi del Molise, Campobasso, Italy  
Università degli Studi di Torino, Turin, Italy  
Università di Udine, Udine, Italy

#### **Foreign Institutions**

Université Libre de Bruxelles, Brussels, Belgium  
Universidade Federal de Sao Paulo, Brazil  
University of Turku, Turku, Finland  
Université Paris Sud XI, Paris, France  
University of Madras, Chennai, India  
University Pavol Jozef Šafàrik, Kosice, Slovakia  
Universidad Autonoma de Madrid, Centro de Investigaciones Oncologicas (CNIO), Spain  
Johns Hopkins School of Medicine, Baltimore, MD, USA  
Johns Hopkins Krieger School of Arts and Sciences, Baltimore, MD, USA  
National Institutes of Health, Bethesda, MD, USA  
Ohio State University, Columbus, OH, USA  
Albert Einstein College of Medicine of Yeshiwa University, N.Y., USA

#### **Supporting Institutions**

Associazione Leonardo di Capua, Naples, Italy  
Dipartimento di Biologia e Patologia Cellulare e Molecolare “L. Califano”, Università degli Studi di Napoli “Federico II”, Naples, Italy  
Istituto Superiore di Oncologia (ISO), Genoa, Italy  
Istituto di Endocrinologia ed Oncologia Sperimentale “G. Salvatore”, CNR, Naples, Italy

## Italian Faculty

Giancarlo Vecchio, MD, Co-ordinator	Antonio Leonardi, MD
Salvatore Maria Aloj, MD	Paolo Emidio Macchia, MD
Francesco Saverio Ambesi Impiombato, MD	Barbara Majello, PhD
Francesco Beguinot, MD	Rosa Marina Melillo, MD
Maria Teresa Berlingieri, MD	Claudia Miele, PhD
Bernadette Biondi, MD	Roberto Pacelli, MD
Francesca Carlomagno, MD	Giuseppe Palumbo, PhD
Gabriella Castoria, MD	Silvio Parodi, MD
Angela Celetti, MD	Nicola Perrotti, MD
Lorenzo Chiariotti, MD	Giuseppe Portella, MD
Vincenzo Ciminale, MD	Giorgio Punzo, MD
Annamaria Cirafici, PhD	Antonio Rosato, MD
Annamaria Colao, MD	Guido Rossi, MD
Sabino De Placido, MD	Giuliana Salvatore MD
Gabriella De Vita, MD	Massimo Santoro, MD
Monica Fedele, PhD	Giampaolo Tortora, MD
Pietro Formisano, MD	Donatella Tramontano, PhD
Alfredo Fusco, MD	Giancarlo Troncone, MD
Michele Grieco, MD	Giuseppe Viglietto, MD
Massimo Imbriaco, MD	Mario Vitale, MD
Paolo Laccetti, PhD	

## Foreign Faculty

### *Université Libre de Bruxelles, Belgium*

Gilbert Vassart, MD  
Jacques E. Dumont, MD

### *Universidade Federal de Sao Paulo, Brazil*

Janete Maria Cerutti, PhD  
Rui Monteiro de Barros Maciel, MD PhD

### *University of Turku, Turku, Finland*

Mikko Laukkanen, PhD

### *Université Paris Sud XI, Paris, France*

Martin Schlumberger, MD  
Jean Michel Bidart, MD

### *University of Madras, Chennai, India*

Arasambattu K. Munirajan, PhD

### *University Pavol Jozef Šafárik, Kosice, Slovakia*

Eva Cellárová, PhD  
Peter Fedoročko, PhD

### *Universidad Autonoma de Madrid - Instituto de Investigaciones Biomedicas, Spain*

Juan Bernal, MD, PhD  
Pilar Santisteban, PhD

### *Centro de Investigaciones Oncologicas, Spain*

Mariano Barbacid, MD

### *Johns Hopkins School of Medicine, USA*

Vincenzo Casolaro, MD  
Pierre A. Coulombe, PhD  
James G. Herman MD  
Robert P. Schleimer, PhD

### *Johns Hopkins Krieger School of Arts and Sciences, USA*

Eaton E. Lattman, MD

### *National Institutes of Health, Bethesda, MD, USA*

Michael M. Gottesman, MD

J. Silvio Gutkind, PhD  
Genoveffa Franchini, MD  
Stephen J. Marx, MD  
Ira Pastan, MD  
Phillip Gorden, MD

### *Ohio State University, Columbus, OH, USA*

Carlo M. Croce, MD  
Ginny L. Bumgardner, MD PhD

### *Albert Einstein College of Medicine of Yeshiwa University, N.Y., USA*

Luciano D'Adamio, MD  
Nancy Carrasco, MD

**“PED/PEA-15 regulates wound healing and angiogenesis by affecting cytoskeletal organization and cell motility: a model for diabetic complications”**

## TABLE OF CONTENTS

<b>1. BACKGROUND</b>	4
1.1 Diabetes	4
1.1.2 Type 1 Diabetes Mellitus	4
1.1.3 Type 2 Diabetes Mellitus	5
1.1.4 Metabolic abnormalities	5
1.2 Genetic consideration	6
1.3 Hyperglycemia and diabetic complication	7
1.4 Diabetic foot	8
1.4.1 Wound healing physiology	8
1.5 Molecular mechanism of wound healing	10
1.5.1 Cell proliferation	10
✓ RAS/MAPK pathway	10
✓ PKCS' pathway	11
✓ PI3K/PKB pathway	12
1.5.2 Cell migration	12
✓ JNK signalling	14
✓ p38 signaling	15
✓ ERK/MAPK signalling	15
1.6 Wound healing in diabetes	16
1.6.1 The inflammatory component of diabetic wound healing	17
1.6.2 Fibroblasts dysfunction in diabetes	19
<b>2. AIM OF THE STUDY</b>	20
<b>3. MATHERIALS AND METHODS</b>	21
<b>4. RESULTS AND DISCUSSION</b>	27
4.1 Ped/Pea-15 effect on wound healing in vivo	27
4.2 <i>In vivo</i> evaluation of mice inflammatory state	27
4.3 Assessment of angiogenetic resonse in mice skin	28
4.4 Effect of Ped/Pea-15 on endothelial cells migration and tube formation	28
4.5 Effect of Ped/Pea-15 on fibroblasts involved in the wound healing	30
4.6 Direct evaluation of fibroblast motility by time-lapse microscopy (TLM)	32
4.7 Ped/Pea-15 effect on cell adhesion, spreading and cytoskeleton organization	34
4.8 Ped/Pea-15 effect on RhoA activity and subcellular distribution	35
4.9 Ped/Pea-15 effect on ERK1/2 activation and function in wound healing alteration	36
4.10 Ped/Pea-15 depletion increased fibroblast, spreading and wound closure	40
<b>5. CONCLUSIONS</b>	42
<b>6. ACKNOWLEDGMENTS</b>	44
<b>7. REFERENCES</b>	45

## LIST OF PUBLICATIONS

This dissertation is based upon the following publications:

Roberta Buonomo<sup>\*1,2</sup>, Ferdinando Giacco<sup>\*1,2</sup>, Angela Vasaturo<sup>3</sup>, Stefano Guido<sup>3</sup>, Corrado Garbi<sup>1</sup>, Valentina Pagliara<sup>1</sup>, Gelsomina Mansueto<sup>4</sup>, Angela Cassese<sup>1,2</sup>, Giuseppe Perruolo<sup>1,2</sup>, Francesco Oriente<sup>1</sup>, Claudia Miele<sup>1,2</sup>, Francesco Beguinot<sup>1,2</sup>, Pietro Formisano<sup>1,2</sup>.

***Phosphoprotein enriched in diabetes/phosphoprotein enriched in astrocytes-15 controls fibroblast migration and wound closure by an extracellular signal-regulated kinase 1/2-dependent mechanism***

The Journal of Biological Chemistry, Pending revision

R. Buonomo, A. Cassese, F. Giacco, G. Raciti, Claudia Miele, Pietro Formisano, Francesco Beguinot

***Ped/pea-15 ablation in vivo ameliorates glucose stimulated insulin secretion and increases glucose tolerance in mice***

Manuscript in preparation.

## ABSTRACT

Failure in wound healing is a common feature of diabetes mellitus which severely affects morbidity and mortality. We evaluated wound healing in the skin of transgenic mice (TgPED) over-expressing *ped/pea-15*, a gene over-expressed in patients with type 2 diabetes. Up to four days after the injury, the distance between wound edges was 3-fold higher in TgPED mice compared to their wild-type littermates (Wt). TgPED mice also presented significantly reduced granulation tissue formation as compared to Wt. Moreover, the wounded skin of TgPED exhibited also a reduced content of activated fibroblasts, collagen fibres and an increased detection of infiltrated inflammatory cells. These histological alterations were accompanied, in TgPED specimens, by an increased production of inflammatory cytokines and a defect of neo-angiogenesis process. Then we isolated endothelial cells and fibroblasts from TgPED and Wt mice, mainly involved in the formation of the granulation tissue, the first regenerative tissue that closes the skin gap. Endothelial cells and skin fibroblasts isolated from TgPED and Wt mice showed reduced healing ability in scratch wound healing assays compared to control cells. Furthermore, in time-lapse experiments, TgPED fibroblasts displayed about 2-fold lower velocity and diffusion coefficient, as compared with Wt. These changes were accompanied by reduced spreading and decreased formation of stress fibres and focal adhesion plaques. At molecular level, TgPED fibroblasts displayed decreased RhoA membrane content and increased cytosolic abundance of phosphorylated ERK1/2. Inhibition of ERK1/2 activity by PD98059 restored RhoA membrane translocation, cytoskeleton organization and cell motility and almost completely rescued wound healing ability of TgPED fibroblasts and can be expanded to endothelial cells. Interestingly, fibroblasts isolated from *ped/pea-15* null mice (KO) displayed an increased motility and spreading compared to control cells. These results strongly support a role of PED/PEA-15 in the regulation of cell motility during skin wound healing. Moreover, the control exerted by PED/PEA-15 on cell migration is not restricted to fibroblasts. Considering the different known cellular function of PED/PEA-15 in a chronic disorder such as diabetes, the observation that PED/PEA-15 regulates cellular motility and skin wound healing in TgPED mice may suggest these mice as model to study the role of PED/PEA-15 in diabetic complications.

# **1. BACKGROUND**

## **1.1 Diabetes**

Diabetes mellitus (DM) comprises a group of common metabolic disorders that share the phenotype of hyperglycemia. Several distinct types of DM exist and are caused by a complex interaction of genetic and environmental factors, and lifestyle choices. Depending on the etiology of the DM, factors contributing to hyperglycemia may include reduced insulin secretion, decreased glucose utilization, and increased glucose production. The metabolic dysregulation associated with DM causes secondary pathophysiologic changes in multiple organ systems that impose a tremendous burden on the individual with diabetes and on the health care system. DM is classified on the basis of the pathogenic process that leads to hyperglycemia. The two broad categories of DM are designated type 1 and type 2. Type 1A DM results from autoimmune beta cell destruction, which leads to insulin deficiency. Individuals with type 1B DM lack immunologic markers indicative of an autoimmune destructive process of the beta cells. However, they develop insulin deficiency by unknown mechanisms and are ketosis prone. Relatively few patients with type 1 DM are in the type 1B idiopathic category. Type 2 DM is a heterogeneous group of disorders characterized by variable degrees of insulin resistance, impaired insulin secretion, and increased glucose production. Distinct genetic and metabolic defects in insulin action and/or secretion give rise to the common phenotype of hyperglycemia in type 2 DM (Harrison 2009).

### **1.1.2 Type 1 diabetes mellitus**

Type 1A DM develops as a result of the synergistic effects of genetic, environmental, and immunologic factors that ultimately destroy the pancreatic beta cells. Individuals with a genetic susceptibility have normal beta cell mass at birth but begin to lose beta cells secondary to autoimmune destruction that occurs over months to years. This autoimmune process is thought to be triggered by an infectious or environmental stimulus and to be sustained by a beta cell-specific molecule. In the majority of individuals, immunologic markers appear after the triggering event but before diabetes becomes clinically overt. Beta cell mass then begins to decline, and insulin secretion becomes progressively impaired, although normal glucose tolerance is maintained. The rate of decline in beta cell mass varies widely among individuals, with some patients progressing rapidly to clinical diabetes and others evolving more slowly. Features of diabetes do not become evident until a majority of beta cells are destroyed (80%) and the individual becomes completely insulin deficient (Harrison 2009). Genetic susceptibility to

type 1A DM involves multiple genes. The major susceptibility gene for type 1A DM is located in the HLA region on chromosome 6. Polymorphisms in the HLA complex account for 40 to 50% of the genetic risk of developing type 1A DM. Most individuals with type 1A DM have the HLA DR3 and/or DR4 haplotype. Refinements in genotyping of HLA loci have shown that the haplotypes DQA1\*0301, DQB1\*0302, DQA1\*501, and DQB1\*0201 are most strongly associated with type 1A DM. The risk of developing type 1A DM is increased tenfold in relatives of individuals with the disease. Nevertheless, most individuals with predisposing haplotypes do not develop diabetes. In addition, most individuals with type 1A DM do not have a first-degree relative with this disorder (Harrison 2009).

### **1.1.3 Type 2 diabetes mellitus**

Type 2 DM is characterized by three pathophysiologic abnormalities: impaired insulin secretion, peripheral insulin resistance, and excessive hepatic glucose production. Obesity, particularly visceral or central (as evidenced by the hip-waist ratio), is very common in type 2 DM. In the early stages of the disorder, glucose tolerance remains normal, despite insulin resistance, because the pancreatic beta cells compensate by increasing insulin output. As insulin resistance and compensatory hyperinsulinemia progress, the pancreatic islets in certain individuals are unable to sustain the hyperinsulinemic state. Then develops impaired glucose tolerance, characterized by elevations in postprandial glucose. A further decline in insulin secretion and an increase in hepatic glucose production lead to overt diabetes with fasting hyperglycemia. Ultimately, beta cell failure may ensue (Harrison 2009).

### **1.1.4 Metabolic abnormalities**

*Insulin resistance:* The decreased ability of insulin to act effectively on peripheral target tissues (especially muscle and liver) is a prominent feature of type 2 DM and results from a combination of genetic susceptibility and obesity. Insulin resistance is relative, however, since supernormal levels of circulating insulin will normalize the plasma glucose. Insulin dose-response curves exhibit a rightward shift, indicating reduced sensitivity, and a reduced maximal response, indicating an overall decrease in maximum glucose utilization (30 to 60% lower than normal individuals). Insulin resistance impairs glucose utilization by insulin-sensitive tissues and increases hepatic glucose output; both effects contribute to the hyperglycemia. Increased hepatic glucose output predominantly accounts for increased fasting plasma glucose levels, whereas decreased peripheral glucose usage results in postprandial hyperglycemia. The precise molecular mechanism of

insulin resistance in type 2 DM has not been elucidated. Insulin receptor levels and tyrosine kinase activity in skeletal muscle are reduced, but these alterations are most likely secondary to hyperinsulinemia and are not a primary defect. Therefore, post-receptor defects are believed to play the predominant role in insulin resistance. Another emerging theory proposes that elevated levels of free fatty acids, a common feature of obesity, may contribute to the pathogenesis of type 2 DM. Free fatty acids can impair glucose utilization in skeletal muscle, promote glucose production by the liver, and impair beta cell function (Harrison 2009).

*Impaired insulin secretion:* Insulin secretion and sensitivity are interrelated. In type 2 DM, insulin secretion initially increases in response to insulin resistance to maintain normal glucose tolerance. In the beginning, the insulin secretory defect is mild and selectively involves glucose-stimulated insulin secretion. The response to other nonglucose secretagogues, such as arginine, is preserved. Eventually, the insulin secretory defect progresses to a state of grossly inadequate insulin secretion. The reason(s) for the decline in insulin secretory capacity in type 2 DM is unclear. The metabolic environment of diabetes may also negatively impact islet function. For example, chronic hyperglycemia paradoxically impairs islet function (“glucose toxicity”) and leads to a worsening of hyperglycemia. In addition, elevation of free fatty acid levels (“lipotoxicity”) and dietary fat may also worsen islet function.

*Increased hepatic glucose production:* In type 2 DM, insulin resistance in the liver rejects the failure of hyperinsulinemia to suppress gluconeogenesis, which results in fasting hyperglycemia and decreased glycogen storage by the liver in the postprandial state. Increased hepatic glucose production occurs early in the course of diabetes, though likely after the onset of insulin secretory abnormalities and insulin resistance in skeletal muscle.

## **1.2 Genetic consideration**

Polymorphisms in IRS-1 may be associated with glucose intolerance, raising the possibility that polymorphisms in various postreceptor molecules may combine to create an insulin-resistant state. The pathogenesis of insulin resistance is currently focused on a PI-3-kinase signaling defect, which reduces translocation of GLUT4 to the plasma membrane, among other abnormalities. Of note, not all insulin signal transduction pathways are resistant to the effects of insulin [e.g., those controlling cell growth and differentiation and using the mitogen-activated protein (MAP) kinase pathway]. A common aminoacid polymorphism of PPAR $\gamma$  (*peroxisome proliferator-activated receptor- $\gamma$* ) has been associated to type 2 diabetes (Altshuler et al. 2000). Individuals homozygotes for Pro12 allele are more insulin resistant and present a risk of development of T2D 1,25 times higher than heterozygotes for alleles Ala12/Pro12. Modifications of Calpain-10 gene have been also associated to T2D.

Affected people have an increase of 3 times in risk of development of T2DM. These modifications affect both beta cell function and insulin function on muscle and adipose tissue (Horikawa et al 2000). The Phosphoprotein Enriched in Diabetes/ Phosphoprotein Enriched in Astrocytes-15 (PED/PEA-15) is a 15 kDa cytosolic protein widely expressed in different tissues and highly conserved among mammals, whose gene maps on human chromosome 1q21-22 (Estellès et al. 1996). Overexpression of the PED/PEA-15 gene is a common defect in type 2 diabetes. During a study using a differential display technique to identify genes whose expression was altered in type 2 diabetes, it has been demonstrated that both PED/PEA-15 mRNA and protein levels were overexpressed in fibroblasts from type 2 diabetics compared with non-diabetic individuals. Also skeletal muscle and adipose tissues, two major sites of insulin resistance in type 2 diabetes, showed the same behaviour (Condorelli et al. 1998). Furthermore, a recent study showed that PED/PEA-15 overexpression represents a common abnormality in both T2 DM and their First Degree Relatives (FDR) (Valentino et al. 2006). Cells overexpressing PED/PEA-15 showed an impaired insulin-dependent glucose uptake. Transgenic mice overexpressing PED/PEA-15 exhibit mildly elevated random-fed blood glucose levels and become hyperglycemic after glucose loading, indicating that increased expression of this gene is sufficient to impair glucose tolerance. Moreover, transgenic mice become diabetic after administration of high-fat diets, indicating that, *in vivo*, the overexpression of PED/PEA-15 in conjunction with environmental modifiers may lead to diabetes (Vigliotta et al. 2004). Thus, these findings identify PED/PEA-15 as a novel gene controlling insulin action contributing, under appropriate environmental conditions, to genetic susceptibility to type 2 diabetes in humans.

### **1.3 Hyperglycemia and diabetic complication**

Type 1 DM and type 2 DM share the phenotype of hyperglycemia. Prolonged hyperglycemia is responsible for the onset of diabetic complications. Four main hypotheses about how hyperglycaemia causes diabetic complications have been generated. The four hypotheses based on distinct biochemical abnormalities are: increased polyol pathway flux; increased advanced glycation end-product (AGE) formation; activation of protein kinase C (PKC) isoforms; and increased hexosamine pathway flux (for further details see: Brownlee 2001). In human diabetes, the resulting problems are grouped under "microvascular disease" (due to damage to small blood vessels) and "macrovascular disease" (due to damage to the arteries). The damage to small blood vessels leads to a microangiopathy, which can cause one or more of the following: retinopathy, neuropathy, or nephropathy. Macrovascular disease leads to cardiovascular disease, to which accelerated atherosclerosis is a contributor of coronary artery disease, leading to angina or

myocardial infarction, stroke, peripheral vascular disease, diabetic myonecrosis ('muscle wasting') or diabetic foot (Harrison 2009).

#### **1.4 Diabetic foot**

Diabetic foot ulcers (DFUs), a leading cause of amputations, affect 15% of people with diabetes. A series of multiple mechanisms, including decreased cell and growth factor response, lead to diminished peripheral blood flow and decreased local angiogenesis, all of which can contribute to lack of healing in persons with DFUs. Most commonly, patients have neuropathy, which could be causative. When coupled with an impaired ability to fight infection, these patients become largely unable to mount an adequate inflammatory response. Thus, the DFU that may look like a healing wound becomes a portal for infection that can lead to sepsis and require limb amputation. Over 100 known physiologic factors contribute to wound healing deficiencies in individuals with diabetes. These include decreased or impaired growth factor production (Galkowska et al.2006), angiogenic response (Galiano et al. 2004), macrophage function (Maruyama et al. 2007), collagen accumulation, epidermal barrier function, quantity of granulation tissue, keratinocyte and fibroblast migration and proliferation, number of epidermal nerves (Gibran et al. 2002), bone healing, and balance between the accumulation of ECM components and their remodeling by matrix metalloprotease (MMPs) (Lobman et al. 2002). Wound healing occurs as a cellular response to injury and involves activation of keratinocytes, fibroblasts, endothelial cells, macrophages, and platelets. Many growth factors and cytokines released by these cell types are needed to coordinate and maintain healing.

##### **1.4.1 Wound healing physiology**

Wound healing is often artificially compartmentalized into three phases. None of these phases correspond to a precisely defined period of time, and all phases overlap to a certain degree. They are the inflammatory phase, the proliferative phase, and the maturational phase (Falanga 2005). The inflammatory phase is characterized by hemostasis and inflammation. Wound healing begins with the formation of a fibrin plug consists of platelets embedded in a meshwork of mainly polymerised fibrinogen (fibrin), fibronectin, vitronectin, and thrombospondin; it is an immediate way to ward off bacteria and provide temporary wound coverage. Within the plug, platelets aggregate and release a wide range of growth factors, including platelet-derived growth factor (PDGF) and transforming growth factor (TGF)  $\beta$ 1, fibroblasts growth factor (FGF-2), vascular endothelial growth factor (VEGF), hepatocyte growth factor (HGF), insulin growth factor (IGF), epidermal growth factor (EGF), and sphingosine-1-phosphate (S1P). Together, this growth factors influences many cells, including fibroblasts, keratinocytes, and endothelial

cells (Baum et al 2005). The ingress of Polymorphonuclear cells (PMNs) to the injured area initiates the inflammatory phase. PMNs serve as early “cleaners” of the wound by removing cellular debris, foreign particles, and bacteria (Lawrence 1998). They are a major source of several proinflammatory cytokines, such as IL-1 $\alpha$ , IL-1 $\beta$ , IL-6, and tumor necrosis factor (TNF)- $\alpha$  (Werner et al 2003). After PMNs at the wound site arrive macrophages that also remove debris, foreign particles, bacteria and secrete a number of growth factors and cytokines (Baum et al 2005). The inflammatory process is perpetuated through macrophage production of proinflammatory cytokines (Hubner et al 1996).

The second stage of wound healing is the proliferative phase. Granulation tissue formation, migration, production of extracellular matrix (ECM), angiogenesis, and reepithelialization are the principal steps in this anabolic portion of wound healing. The components of the granulation tissue include fibroblasts, collagen (produced by fibroblasts) and blood vessels. Fibroblasts are the most important mesenchymal cells involved in wound healing (Lawrence 1998) given their dual roles of “factory” and “machinery.” As factories, fibroblasts produce the collagen-based ECM. As “machinery,” fibroblasts help reapproximate wound edges through their contractile properties. The processes of migration, proliferation, and ECM production are the key steps in the regeneration of a functional dermis. The increase in fibroblast population in the provisional ECM is due to the influx of migrating cells in addition to the proliferation of cells and is stimulated by PDGF, NGF, TGF- $\beta$ , CTGF, and cysteine-rich 61 (Cyr61). Two of the “factory-like” roles of fibroblasts include the production of a permanent ECM (including collagen, glycosaminoglycan [GAG], and proteoglycans) and growth factors, which regulate the function of other cells in the matrix (Baum et al 2005).

Angiogenesis is the process by which damaged blood vessels are replaced by “sprouts” from intact capillaries in the local vicinity of the wound. Several growth factors and cytokines, produced during the inflammatory phase of wound healing, stimulate and regulate angiogenesis. Endothelial cells migrate into the wound along the provisional ECM in a manner similar to that of fibroblasts (Senger et al. 1996). Endothelial migration is stimulated by VEGF, FGF, angiopoietin, and TGF- $\beta$  (Baum et al 2005). The ECM influences angiogenesis. Together, the various components of the ECM, such as fibronectin, collagen, and vitronectin, provide structural support for the invading capillaries, in addition to serving as a repository of important growth factors, such as FGF-2 and TGF- $\beta$  (Witt and Lander 1994)

The gross morphologic changes that occur during reepithelialization include sloughing of any residual eschar and, ultimately, the reestablishment of intact epidermis over granulation tissue. As the process of reepithelialization progresses, a mass of keratinocytes moves across the granulation tissue. At the leading edge of the wedge are migrating keratinocytes, which leave a stratified layer of proliferating keratinocytes in their wake. This process, known as contact guidance,

continues until keratinocytes from opposing sides of the wound reestablish contact. Keratinocytes are stimulated to migrate, proliferate, and eventually differentiate by a number of factors. FGF-2, FGF-7, FGF-10, and TGF- $\beta$  demonstrate a positive influence on migration; HB-EGF, HGF, NGF, IL-6, GM-CSF, nitric oxide, leptin, and secretory domain of  $\beta$ -amyloid precursor protein (sAPP) demonstrate a positive influence on cell proliferation (Baum et al 2005). The final phase of wound healing is the maturational phase. The clinical manifestations of wound maturation include contraction, decreased redness, thickness, induration, and increased strength. Fibroblasts and their products, collagen and MMPs, along with blood vessels, constitute the main participants in wound maturation. At this stage, the wounded skin regains its strength and elasticity, and proceeds through reorganization of the collagen and elastic fibers for final reconstruction of the dermis. The scar-tissue formation marks the termination of the healing process since all of the other assessed parameters have returned to prewounding levels and distribution (Braithwaite-Wiksman et al 2007).

## **1.5 Molecular mechanism of wound healing**

Wound healing involves a complex interaction and equilibrium of cells, cytokines and growth factors working in concert. Two major cellular functions are necessary for a proper wound healing: cell proliferation and motility.

### **1.5.1 Cell proliferation**

Fundamental part of the answer to the damage in the process of wound healing is the cellular proliferation. The mostly interested cells are fibroblasts and the endothelial cells. Cell proliferation is triggered by the binding of a messenger molecule to a specific receptor of the target cell. In mammalian cells the cascade often is begun from the activation of a receptor with intrinsic tyrosin-kinase activity by interaction with a growth factor, such as EGF, FGF, PDGF and IGF-1. The interaction with the ligand induces the dimerization of the receptor and the autophosphorylation on tyrosine residues. Phosphorylated tyrosines represent site of protein-protein interaction and act as activation site for intracellular proteins responsible for transduction of the signal from the cellular surface to the nucleus. In particular, there are three main pathways of signalling that have a primary role in the stimulation of the cellular proliferation.

- *RAS/MAPK pathway*

Receptor-linked tyrosine kinases such as the epidermal growth factor receptor (EGFR) are activated by extracellular ligands. Binding of EGF to the EGFR activates the tyrosine kinase activity of the cytoplasmic domain of the receptor.

The EGFR becomes phosphorylated on tyrosines. Docking proteins such as GRB2 contain SH2 domains that bind to the phosphotyrosines of the activated receptor (Shulze et al. 2005). GRB2 binds to the guanine nucleotide exchange factor SOS by way of an SH3 domain of GRB2. When the GRB2-SOS complex docks to phosphorylated EGFR, SOS becomes activated (Zarich et al. 2006). Activated SOS promotes the removal of GDP from Ras. Ras can then bind GTP and become active. Activated Ras activates the protein kinase activity of RAF kinase (Avruch 2001), a serine/threonine-selective protein kinase. RAF kinase phosphorylates and activates MEK, another serine/threonine kinase. MEK phosphorylates and activates Extracellular Signal-regulated kinase 1e 2 (Erk 1/2). Active Erk 1/2 translocates into the nucleus and phosphorylates several transcription factors stimulating cell proliferation (Figure 1).

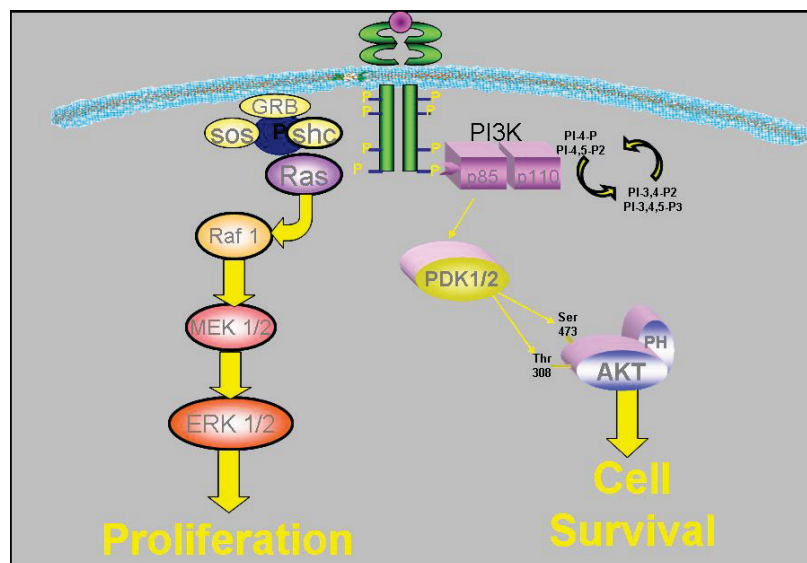


**Figure 1.** Erk 1/2 and Akt/PKB pathway in cell proliferation.

• *PKCS' pathway*

PKCs proteins belong to a multigenic family including at least 14 isoforms with different catalytic and regulatory proprieties (Schmeichel et al 2003). PKCs can be divided in three subgroups on the basis of their structural features and cofactor dependency. Classical PKCs ( $\alpha$ ,  $\beta$ I,  $\beta$ II and  $\gamma$ ) are  $Ca^{2+}$  and diacylglycerol (DAG) dependent; novel PKCs ( $\delta$ ,  $\epsilon$ ,  $\eta$ ,  $\theta$ ) are DAG dependent but are  $Ca^{2+}$  independent; the atypical PKCs ( $\zeta$ ,  $\lambda$  e  $\iota$ ) are both  $Ca^{2+}$  and DAG independent. PKCs play an important role in several cellular functions such as proliferation, metabolism, vesicular traffic and cytoskeleton organization. In response to growth factors one of the mechanisms of PKCs activation is mediated by phospholipase C e D production of DAG.

• *PI3K/PKB pathway*

PI3K family includes several isoforms divided in three classes based on structural features and regulation mechanisms (Schlessinger 1993). The most known class is the Ia that is activated in response to growth factors. Class Ia consisting of heterodimers composed of a 85 kDa regulatory subunit (p85) and of a 110 kDa lipidic kinase catalytic subunit (p110). Interaction of p85 with phosphorylated tyrosines on activated growth factors receptors or on adapting proteins induces a conformational change that modulates p110 catalytic activity (Goalstone 1998).

Activated PI3K phosphorylates the membrane lipid phosphatidylinositol on 3' position of inositolic ring inducing an increase of phosphatidylinositol 3-phosphate (PI3P), of phosphatidylinositol 3, 4-biphosphate (PI3,4P2) and of phosphatidylinositol 3,4,5 tri-phosphate (PI3,4,5P3). Phosphorylated phosphatidylinositol act as second messenger and mediate PI3K effect on cytoskeleton, cell cycle, vesicular traffic, glucose metabolism and cell survival. Phospholipid activated proteins include some  $Ca^{+2}$ -independent PKC isoforms, such as PKC $\delta$  and PKC $\zeta$  (Blumberg et al 1996), p70S6 kinase, small GTPase Rho and Rac and serine-threonine-kinase PKB/Akt (Jaken 1996) p70S6 kinase phosphorylates 40S ribosomal subunit protein S6, inducing G1-S cell cycle transition; small GTPase Rho and Rac regulate actin cytoskeleton; PKB/Akt phosphorylates and sequesters into cytosol proapoptotic protein Bad. Thus Bad is unable to associate to Bcl-2 and to translocate into mitochondria to induce cytochrome C release and to trigger apoptotic signal (Cantrell 2001) (Figure 2).

### 1.5.2 Cell migration

Cell migration at wound site is another fundamental event in wound healing process. The crawling movements of animal cells are among the most difficult to explain at the molecular level. Different parts of the cell change at the same time, and there is not a single, easily identifiable locomotory organelle (analogous to a flagellum, for example). Although actin forms the basis of animal cell migration, it undergoes many different transformations as the cell moves forward, assembling into lamellipodia and microspikes, associating with focal contacts, forming stress fibers, and so on. In broad terms, three distinct processes can be identified in the crawling movements of animal cells: protrusion, in which lamellipodia and microspikes (or filopodia) are extended from the front of the cell; attachment, where the actin cytoskeleton makes a connection with the substratum; and traction, where the body of the cell moves forward. Protrusion is a function of the leading edge of the cell. Actin-rich lamellipodia and microspikes (or filopodia) extend forward over the substratum, a process that is accompanied by actin polymerization. It seems likely that the protrusion is driven by actin polymerization at the leading edge, although this is still debated. Myosin-I motors

attached to the plasma membrane could also drive the cell forward by actively walking along actin filaments. Rapidly motile cells, such as white blood cells, make more diffuse contacts with the substratum. It is thought, however, that similar principles apply to focal contacts of fibroblasts: transmembrane receptors for extracellular matrix proteins link the plasma membrane to the substratum, and actin filaments in the cytoplasm interact with the cytoplasmic domains of these receptors through actin-binding proteins. The details of these important interactions are uncertain, but it is clear that the cell contacts with the substratum must be continually made and broken as the cell moves forward. The dynamic assembly and disassembly of focal adhesions plays a central role in cell migration. During cell migration, both the composition and the morphology of the focal adhesion changes. Initially, small ( $0.25\mu\text{m}^2$ ) focal adhesions called "focal complexes" are formed at the leading edge of the cell in lamellipodia: they consist of integrin, and some of the adapter proteins, such as talin and paxilin. Many of these focal complexes fail to mature and are disassembled as the lamellipodia withdraws. However, some focal complexes mature into larger and stable focal adhesions, and recruit many more proteins such as zyxin. Once in place, a focal adhesion remains stationary with respect to the ECM, and the cell uses this as an anchor on which it can push or pull itself over the ECM. As the cell progresses along its chosen path, a given focal adhesion moves closer and closer to the trailing edge of the cell. At the trailing edge of the cell the focal adhesion must be dissolved. The mechanism of this is poorly understood and is probably instigated by a variety of different methods depending on the circumstances of the cell. Traction is perhaps the most mysterious part of cell locomotion. In many cases it is thought that the force for cell locomotion is generated near the front of the cell and that the nucleus and bulk cytoplasm are dragged forward passively. The force generation can be viewed in different ways. The leading part of the cell might actively contract like a muscle fiber and thus pull on the back of the cell. In another view polymerization of actin filaments at the front of the cell extends the actin cortex forward, and the rear of the cell is then carried forward by the contractile force of the resulting cortical tension (Figure 2) (Alberts).

Also cell motility is triggered by binding of signal molecules to specific receptors on cell surface. Ligand-receptor interaction activates several pathways of transduction inside the cell inducing rearrangement in cytoskeleton in order to promote migration. Mitogen activated protein kinase (MAPK) pathway is one of the most important signalling systems in cell migration. In particular, JNK (Jun N-terminus kinase), p38 and ERKs play a pivotal role (Huang et al 2004).

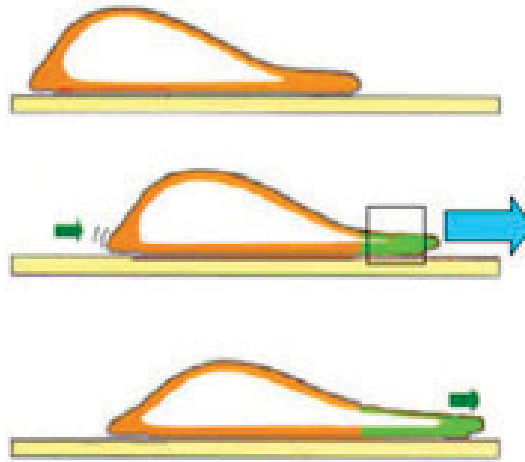


**Figure 2.** Cell movement model

• *JNK signaling*

JNK is activated in response to various extracellular stimuli, including TNF, EGF, PDGF, TGF- $\beta$  and lysophosphatidic acid, as well as diverse environmental stresses (Huang et al 2004). These activate MAPKKKs: such as MEKK1 and MLK, which phosphorylate and activate two MAPKKs, MKK4 and MKK7. In turn, these phosphorylate the threonine and tyrosine residues within the Thr-Pro-Tyr motif in the JNK activation loop. Accumulating evidence implicates the JNK pathway in regulation of cell migration. First, activation of JNK correlates with an increase in cell migration in several cell types. Second, the signaling molecules that activate JNK are essential for cell migration. MEK kinase 1, an upstream kinase in the JNK pathway, is essential for cell migration and the developmental process of eyelid closure. Third, inhibition of JNK by either the chemical inhibitor SP600125 or the dominantnegative mutant JNK1AF, significantly impairs the rate of migration of several different cell types. Fourth, using a gene knockout approach has been demonstrated that JNK activity plays a crucial role in the migration of fibroblasts in wound healing assays. Active JNK is found in cytoplasmic locations providing evidence for cytoplasmic functions of JNK, in addition to its established nuclear functions. Along with the various well-known transcription factors and apoptosis-related proteins, several cytoskeleton-associated proteins and signaling molecules as well as adaptor proteins have recently been identified as JNK substrates. These include the intermediate filament protein keratin 8, microtubule-associated proteins (MAPs), such as MAP1B, MAP2, DCX and SCG10, the actin-binding protein spir, the protein kinase p90RSK, and the adaptors insulin receptor substrate 1 (Irs-1), p66ShcA and paxillin. Of these, paxillin, spir, DCX, MAP1B and MAP2 are probably directly involved in cell migration. These findings collectively implicate JNK in the control of cell migration in a broad range of cell types and in several developmental processes (Huang et al 2004).

• *p38 signaling*

The activity of p38 is stimulated by many growth factors, cytokines, and chemotactic substances, such as VEGF, FGF, PDGF, TNF, interleukins, lipopolysaccharide (LPS) and formyl-methionylleucyl-phenylalanine (fMLP). The upstream MAPK cascade in this case includes MAPKKKs such as MLK3, DLK and TAK1, which phosphorylate and activate MKK3 and MKK6, which in turn phosphorylate and activate p38. It is well known that p38 is involved in inflammation, apoptosis, cardiomyocyte hypertrophy and cell differentiation. Recently, several studies have suggested it is also involved in the migration of diverse cell types. SB203580 and SB202190, inhibitors of p38, inhibit the migration of smooth muscle cells induced by PDGF, TGF $\beta$  and IL-1 $\beta$ , porcine aortic endothelial cells challenged with PDGF and VEGF, neutrophils stimulated with fMLP, mast cells treated with stem cell factors and antigen, corneal epithelial cells stimulated with hepatocyte growth factor, mouse embryonic fibroblasts challenged with PDGF and IL-1, NMuMG and MDA-MB-231 mammary epithelial cells treated with EGF and TGF $\beta$ 1 and NLT neuronal cells stimulated with Gas6 (encoded by growth arrest-specific gene 6). Moreover, p38AF, a dominant negative mutant of p38, also inhibits the migration of smooth muscle cells induced by PDGF, TGF $\beta$  and IL-1 $\beta$ , NMuMG and MDA-MB-231 mammary epithelial cells in response to EGF and TGF $\beta$ 1 and NLT neuronal cells stimulated with Gas6. Taken together, these findings demonstrate that p38 is involved in growth-factor- and cytokine-induced cell migration (Huang et al 2004).

• *ERK/MAPK signaling*

The Erk MAPKs are the most extensively studied subfamily of MAPKs. Erk has been implicated in the migration of numerous cell types. The Erk pathway inhibitors PD98059 and U0126 inhibit the migration of diverse cell types in response to cell matrix proteins, such as fibronectin, vitronectin and collagen, growth factors such as VEGF, FGF, EGF, insulin and other stimuli, such as fetal calf serum and urokinase plasminogen activator (uPA). Moreover, a dominant negative Erk mutant or inhibition of Erk by an antisense strategy also inhibits cell migration. Erk is thus an important factor in the regulation of cell migration. Erk phosphorylates serine or threonine residues followed by proline. The most stringent consensus sequence is Pro-Leu-Ser/Thr-Pro. Identified substrates include several protein kinases, such as p90rsk, MSK1, MNK1/2, myosin light chain kinase (MCLK) and FAK, the protease calpain, paxillin, as well as transcription factors and nuclear proteins. Of these MCLK, calpain, and FAK are most likely to be involved in Erk-mediated cell migration. Erk regulates FAK-paxillin complex sophisticatedly: initially it promotes complex-assembly by phosphorylation of paxillin and then promote disassembly by subsequent phosphorylation of FAK. It is possible that Erk-modulated disassembly of the FAK-paxillin complex is

involved in focal adhesion disassembly, but its precise role and the mechanism remain to be completely clarified. Erk also participates in cell migration by suppressing the ability of integrins to bind to their extracellular matrix ligands. It is well known that the Ras-Raf- MEK-Erk pathway regulates integrin activation (the affinity of an integrin for its substrate), although the molecular mechanism remains to be elucidated. Because dynamic integrin activation is required for cell migration, Erk might also play an important role regulating cell migration, by regulating integrin activation (Figure 3) (Huang et al 2004).

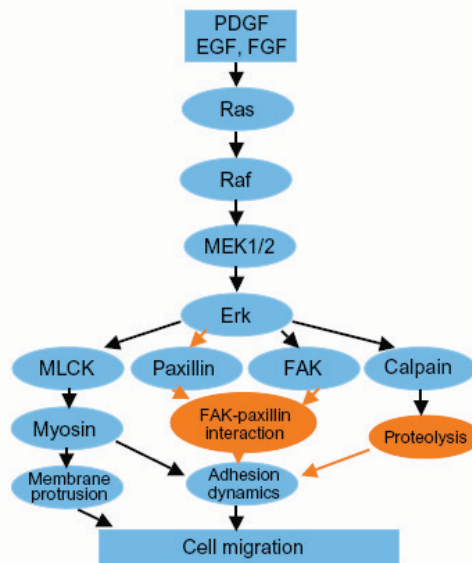


**Figure 3.** Erk 1/2 pathway in cell migration.

### 1.6 Wound healing in diabetes

Diabetic individuals exhibit a documented impairment in the healing of acute wounds, which often develop in chronic non-healing diabetic foot ulcers (DFUs). The impaired healing of both DFUs and acute cutaneous wounds in persons with diabetes involves multiple complex pathophysiological mechanisms. Diabetic ulcers are often stalled in the inflammatory phase with impaired granulation tissue formation and are always accompanied by hypoxia. A situation of prolonged hypoxia is detrimental for wound healing. Indeed, intact and functional microcirculation is necessary for an adequate nutrition of tissues, for discarding metabolism's products and for an effective inflammatory response. Hypoxia can amplify the early inflammatory response, thereby prolonging injury by increasing the levels of oxygen radicals. Hyperglycemia can also add to the oxidative stress when the production of ROS exceeds the anti-oxidant capacity. Several studies have documented an association of the overproduction of these oxygen free

radicals and its deleterious effects on wound healing by perpetuating inflammation, and promoting premature apoptosis of matrix producing cells (Woo et al. 2007). Moreover wound healing is thwarted in the inflammatory stage because ECM is degraded more rapidly than it is synthesized. High levels of metalloproteases are a feature of diabetic foot ulcers, and the MMP levels in chronic wound fluid are almost 60 times higher than those in acute wounds. This increased protease activity supports tissue destruction and inhibits normal repair processes (Sibbald et al. 2008). Increased bacterial burden also plays an important role in the chronicity of ulcers. Impaired host defense occurs at the cellular level where leukocyte function and intracellular killing are both affected, rendering this patient population more susceptible to superficial increased bacterial burden and deep infection (Calhoun et al. 2002; Sibbald et al. 2006). Finally, the diabetic fibroblast response to mitogenic stimulation is often suboptimal with the production of low levels of various growth factors and collagen. Accumulating data demonstrates that persons with diabetes have impaired cell migration and insufficient angiogenesis to support the collagen synthesis necessary for mature granulation and subsequent reepithelialisation (Falanga et al. 2005).

### **1.6.1 The inflammatory component of diabetic wound healing**

The inflammatory response is required for optimal wound healing. Polymorphonuclear neutrophils (PMN) preside at the first wave of immune cells that invade the wound bed and they contribute to the production of inflammatory cytokines (Borst 2004). In contrast to the physiological process, in case of diabetes the inflammatory reaction PMN infiltration is intense and prolonged, sustaining the generation of pro-inflammatory cytokines and a deregulated production of tissue matrix metalloproteinases (MMPs), which sharply limit the process of granulation tissue formation and maturation. Although it is generally accepted that the chronic diabetic ulcer is stalled in the inflammatory phase of the normal healing process, this inflammatory reaction does not necessarily imply a physiological bacterial local control. On the contrary, diabetic individuals are more susceptible to both wound infection and hyperinflammation, which is not pathogenically detachable from the elevated levels of tumour necrosis factor-alpha (TNF- $\alpha$ ) and interleukin (IL)-6 (Borst 2004). The search for explanations on this exaggerated inflammatory reaction has identified critical elements aiming at both soluble and cellular factors. Data derived from diabetic rodent models have documented a prolonged expression of macrophage inflammatory protein-2 (MCP-2) and macrophage chemoattractant protein-1 (MCP-1) (O'Brien et al. 2006). Their dysregulation and sustained expression appears to be directly associated with the increased and protracted infiltration of both PMN and macrophages into the diabetic wound (Wetzler et al 2000). Furthermore the granulocytes secrete pro-

inflammatory cytokines, particularly TNF- $\alpha$  and IL-1b, capable of directly stimulating the synthesis of MMPs, all with a remarkable cytotoxic and prodegradative potential (Schonfelder et al 2005). The observation that diabetic wounds are enriched in MMPs provides support for the premise that impaired growth factor availability may act as a healing and limiting factor (Wetzler et al. 2000). In addition to MMPs, high levels of TNF- $\alpha$  in the wound have been identified as a molecular predictive factor for closure failure (Acosta et al 2008). Type 2 diabetes is associated with high serum levels of inflammatory cytokines such as TNF- $\alpha$  (Mishima et al 2001). Within the wound, TNF- $\alpha$  stimulates its own secretion and that of IL-1b that contributes to a persistent inflammatory status. TNF- $\alpha$  deregulation is also associated to connective tissue destruction, thus pushing towards a catabolic slope (Liu et al. 2006). Genetic ablation of TNF- $\alpha$  receptor-1 improves the general wound healing profile by enhancing angiogenesis, collagen production and reepithelialisation, significantly reducing neutrophil and macrophage infiltration; decreasing gene expression as well as protein levels of IL-1 $\alpha$ , IL-1 $\beta$ , MCP-1, macrophage inflammatory protein-1 alpha (MIP1- $\alpha$ ), and macrophage inflammatory protein-2 (MIP-2); and increased gene expression and protein levels of TGF- $\beta$ 1, connective tissue growth factor (CTGF), and VEGF (Goren et al. 2006). This indicates that TNF- $\alpha$  inhibition is apparently sufficient to neutralise the misbehaving inflammatory machinery in non healing wounds, so as to assist in reprogramming the whole local microenvironment. The effects associated with this intervention include both the restitution of the epithelial sector, as the restoration of granulation tissue outgrowth in terms of cellularity (viability of endothelial cells and fibroblasts), and extracellular matrix synthesis (Liu et al. 2006). Summarising, TNF- $\alpha$  is a major driving force towards the onset and perpetuation of the wound pro-inflammatory and pro-catabolic phenotype. As a concomitant side effect, TNF- $\alpha$  intoxicates fibroblasts and vascular precursor cells. Fibroblasts proliferation and migration are arrested, matrix ingredients secretion is impaired and at the end, these fibroblasts are bound to suicide (Figure 4). An alternative pathogenic cascade establishes a connection between TNF- $\alpha$  levels and tissues insulin resistance from where the skin is not excluded. Systemic TNF- $\alpha$  levels are linked to an impaired healing response under diabetic and obese conditions in ob/ob mice. Chronic exposure of keratinocytes to TNF- $\alpha$  inhibits insulin-stimulated glucose uptake. Indeed TNF- $\alpha$  neutralisation is able to restore insulin sensitivity by reestablishing the expression and functionality of the hormone's receptor (Goren et al. 2006).

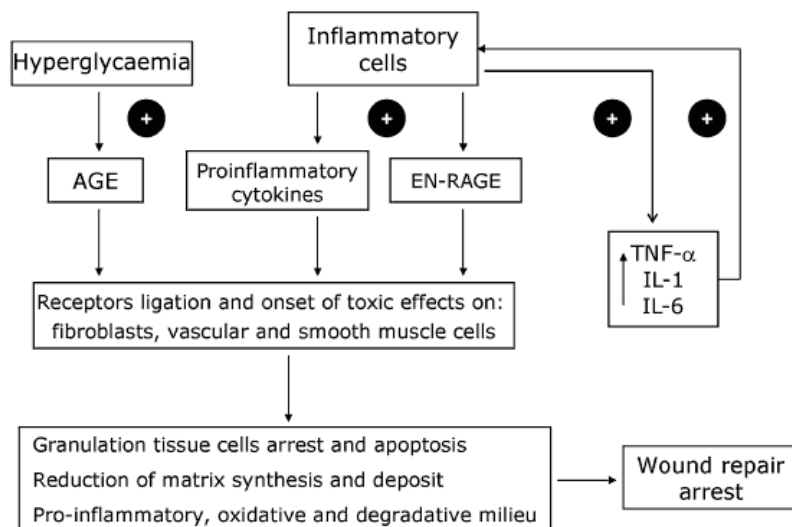


**Figure 4.** The cytotoxic effect of pro-inflammatory cytokines and glycation products in diabetic wound failure.

### 1.6.2 Fibroblasts dysfunction in diabetes

Fibroblasts play a key role in wound healing process. Infact, they produce, secrete and remodel ECM and act as signal cells. It is clear that any impairment of fibroblasts' function induces an impairment in wound healing. In diabetes, in particular, has been demonstrated an impairment in proliferation, migration and ECM synthesis. In detail, diabetic fibroblasts produce and secrete large amount of matrix metalloprotease (MMPs). Physiologically MMPs promote cell migration and healing, nevertheless increased concentration observed in diabetes act as negative regulator of both process. Moreover VEGF production is reduced in diabetic fibroblasts. VEGF is fundamental for vascular development during tissue repair; decreased VEGF levels are responsible for a reduced angiogenetic response that impairs the following proliferation and ECM deposition phases of wound healing. (Lerman et al. 2003).

## 2. AIM OF THE STUDY

Diabetes' incidence is growing up making it one of the most common health problems in western countries. Chronic complications, in particular, cause a significant decrease in life span and life quality of diabetic patients and have a huge cost to public health worldwide. It was calculated that, in 2010, the US spent an estimated \$22.9 billion on direct medical costs related to diabetes complications. A serious complication of diabetes is impaired healing, which can lead to diminished physical activity and in some cases to chronic wounds and limb amputation, having a big impact on life quality and life span of affected patients. Multiple factors contribute to deficient healing in a subset of diabetic patients (Braima-Wiksman 2007, Trousdale et al. 2009). They include altered host response, diminished anti-bacterial defences, prolonged inflammation, altered protease activity, tendency for vascular abnormalities, generation of an inadequate number of cells to accomplish rapid and robust healing, decreased growth factor production, failure to form a sufficient amount of extracellular matrix, and alterations in apoptosis that may interfere with healing by decreasing the number of cells that participate in new tissue formation (Galkowska et al. 2006; Shultz et al. 2009; Wall et al. 2008; Velandar et al. 2008). In particular, fibroblasts play a pivotal role in tissue repair. They function both as synthesizer cells, depositing collagen-rich matrix, and as signalling cells, secreting growth factors important for cell-cell communication during the repair process (Giacco et al 2006). Any impediment to fibroblast functions prevents normal wound closure and results in chronic non-healing wounds. Noteworthy, alterations of fibroblast functions have been reported in individuals with type 2 diabetes (Lerman et al. 2003).

Possibly genetic factors may contribute to wound healing dysregulation in a subset of diabetic patients. *PED/PEA-15* is a gene over-expressed in several tissues and cell types including fibroblasts, of a large cohort of patients with type 2 diabetes (Condorelli et al. 1998; Valentino et al. 2006; Condorelli et al. 2001). *PED/PEA-15* gene product is a ubiquitously expressed protein, which has been implicated in the control of cell survival and growth and glucose metabolism (Fiory et al. 2009). Moreover its over-expression may lead to impaired glucose tolerance in transgenic mice (TgPED). Aim of this work has been to clarify in further detail the sequence of events that characterize the wound healing process in TgPED mice to establish if alteration of this gene may be a predictor factor to development of skin chronic complication in patients affected by diabetes.

## **3. MATERIALS AND METHODS**

### **3.1 Materials**

Tribromoethanol (Avertin<sup>®</sup>) was from Sigma-Aldrich (St. Louis, Mo). Media, sera, and antibiotics for cell culture were purchased from Invitrogen Ltd. (Paisley, United Kingdom). Rabbit polyclonal ERK1/2 and RhoA mouse monoclonal antibodies were from Santa Cruz Biotechnology (Santa Cruz, Calif.), and antibodies toward the phosphorylated forms of ERK1/2 were from Cell Signal Technology (Beverly, Mass). Rabbit polyclonal Paxillin antibodies were from Zymed Laboratories (Invitrogen Corporation, Calif.). Rabbit polyclonal fibronectin antibodies were from Chemicon (Millipore Corporation). Rabbit polyclonal H3-histone and  $\beta$  subunit of the Insulin-like growth factor-1 receptor antibodies were from Upstate (Millipore Corporation). Western blotting, ECL reagents were from Amersham (Arlington Heights, Ill.). Electrophoresis reagents were from BioRad. Rabbit polyclonal  $\beta$ -actin antibodies, Bisindolylmaleimide (BDM), PD98059 and mytomicin C were from Sigma-Aldrich (St. Louis, Mo.)

### **3.2 In vivo wound healing and histological analysis**

We used 16 eight month old, sex and age matched, TgPED and Wt littermates mice for each time point of the study. The animals were anesthetized with a single intraperitoneal injection of tribromoethanol. The hair on the back of each mouse was cut and 2 full-thickness wounds (width about 4 mm, length about 2 cm) were made with scalpel (Braiman-Wiksman 2007). Wounds from all animals were harvested at 3, 4 and 6 days after injury. Samples were fixed in 10% neutral buffered formalin and subsequently processed, blocked and sectioned perpendicularly to the wound surface in 5 $\mu$ m consecutive sections. Healing of skin wounds was evaluated on haematoxylin-eosin (H&E) slides by measuring the distance between migration tongues using the measurement tool included in the digital microscope software. Granulation tissue–staining of proliferating cells with antibodies anti-proliferating cell nuclear antigen (PCNA), collagen fibres with Masson-Trichrom and H&E staining were used to assess the granulation-tissue formation. Granulation tissue was considered fully formed (100%) when the following parameters existed at wound gap: 1) a continuous layer of granulation tissue formed across the entire wound gap; 2) the layer of granulation tissue filled the entire wound depth (Braiman-Wiksman 2007). The inflammatory infiltrate was estimated by immunohistochemical-based quantification of neutrophils, macrophages and T-lymphocytes with anti-neutrophil antibody, anti-CD68 antibody and anti-CD3 antibody, respectively (Hattori et al 2009). PicroSirius Red/Fast Green was used for differential staining of collagen during matrix

production phase. FGF-2 was used for immunohistochemical-based quantification of fibroblast content. All stained samples were examined under digital and light microscope by at least two trained pathologists in blind. The content of activated fibroblasts, infiltrated cells and collagen fibres was scored using a semi-quantitative three point scale of range values. For activated fibroblasts and cellular infiltration, we attributed score 0 for no increase, score 1, 2 or 3 for little, moderate or high increase of cells content compared to adjacent tissue, respectively. For the extracellular matrix production we attributed score 0 for absence of collagen production, score 1 and 2 for 10-40% and 40-80% collagen fibres content compared to adjacent normal tissue respectively, and finally score 3 for wound matrix indistinguishable from adjacent normal tissue. All experiments were performed according to the guidelines and approved by the local Ethic Committee.

### **3.3 Multiplex analysis**

To examine the expression of cytokines during dermal wound healing blood samples of Wt and TgPED mice subjected to skin injury were collected and analyzed. A Bio-Plex conventional assay kit for 27 cytokines was run following the manufacturer's instructions (Bio-Rad Laboratories). Using the Bio-Plex Suspension Array System (Bio-Rad Laboratories) all samples were analyzed in duplicate. The methods were described in detail in the references Takamiya et al. 2008. Furthermore, differences of cytokines expression between blood samples of Wt control and TgPED mice were statistically analyzed using the Student's *t*-test, and P values of 0.05 or less were considered statistically significant.

### **3.4 Directed in vivo angiogenesis assay (DIVAA)**

Sterile, surgical silicone tubing (0.15-cm internal diameter), these are referred to as "angioreactors", were filled at 4°C with 18µl of Matrigel with or without angiogenic factors (500 ng/ml of either FGF-2 and VEGF). These were incubated at 37°C for 1 h to allow gel formation and and were implanted into the dorsal flank of 16 Wt and 16 TgPED mice. At 9 days after implantation, mice received a 100µl injection of 25 mg/ml of FITCdextran in phosphate-buffered saline (PBS) via tail vein. Angioreactors were then recovered at 30 min after intravenous injection. Quantification was performed by removal of the Matrigel and digestion in 200µl of Dispase solution for 1 hour at 37°C. After digestion, the incubation mix was cleared by centrifugation (5 min at 15,000xg) at room temperature and fluorescence of the supernatant aliquots were measured in 96-well plates using an HP model spectrofluorimeter (excitation 485 nm, emission 510 nm). The mean relative fluorescence ± SD for five replicate assays were determined by statistical analysis (Student's *t*-test) (Guedez et al 2003).

### **3.5 Isolation of mouse aortic endothelial cells**

Murine aortic endothelial cells were isolated from cells growing out of tissue explants. TgPED and Wt female mice, 10 week of age, were exsanguinated. The heart and lungs were aseptically removed from the chest cavity and placed in a petri dish containing Hank's balanced salt solution. The aorta was removed from the heart. Connective tissue surrounding the exterior of the vessel was teased away, and the vessel was then washed briefly in HBSS. The aorta was then cut into four or five small segments (1.0-1.5 mm thick). The resulting tissue rings were then placed on edge into a 0.2% gelatin-coated 34-mm tissue culture well and allowed to anchor to the bottom of the well for 2-3 min. The explants were incubated at 37°C after the careful addition of 2 ml of DMEM 20% FBS supplemented with endothelial cells growth supplement (ECGS; Sigma-Aldrich). After sufficient outgrowth of non-fibroblast-like cells, the tissue fragments were removed. The remaining adherent cells were allowed to continue growing. Endothelial cells were identified by di-ID-acylated low-density lipoprotein (di-I-LDL) (Biomedical Technologies Inc., Stoughton, MA) labeling. Isolated endothelial cells were grown at 37°C with DMEM 20% FBS supplemented with ECGS and used between 3 and 8 passages (Lincoln et al. 2003).

### **3.6 Capillary-like tube formation on matrigel**

The EC were made quiescent by contact inhibition and an overnight starvation. After trypsinized, cells were then seeded on Matrigel. Briefly, 100 µl per well of this matrix solution was added to a 24-well culture plate. After gelation at 37 °C for 30 min, EC resuspended in DMEM 20% FBS supplemented with ECGS were plated on the top of the Matrigel at a density of  $5 \times 10^3$  cells/well and incubated for 8 days at 37 °C. Tube formation was observed using an light microscope. Images were captured and the number of the structure were quantified by counting all branches in three random fields from each well. Each experiment was repeated three times (Wang et al. 2009).

### **3.7 Isolation and culture of fibroblasts, Western Blot, Cell fractionation**

TgPED, *ped/pea-15* null (KO) and Wt control mice have been generated and characterized as described previously (Kitsberg et al 1999). Skin fibroblasts were obtained by punch biopsy from the animals. Cultures were established and grown as previously described (Atala and Lanza 2001), and used for experimental procedures between 3 and 10 passages. For Western blotting, the cells were solubilized in lysis buffer (50mM HEPES pH 7.5, 150mM NaCl, 4mM EDTA,

10mM Na<sub>4</sub>PO<sub>7</sub>, 2mM Na<sub>3</sub>VO<sub>4</sub>, 100mM NaF, 10% glycerol, 1% Triton X-100, 1mM phenylmethylsulfonyl fluoride, 100 µg of aprotinin/ml, 1mM leupeptin) for 60 min at 4°C. Lysates were clarified at 5,000 x g for 15 min. Solubilized proteins were then separated by SDS-PAGE and transferred onto 0.45-µm-pore-size Immobilon-P membranes (Millipore, Bedford, Mass.). Upon incubation with the primary and secondary antibodies, immunoreactive bands were detected by ECL according to the manufacturer's instructions. For cell fractions, the cells were solubilized in ice-cold fractionation buffer (20mM HEPES-NaOH, pH 7.4, 250mM sucrose, 25mM sodium fluoride, 1mM sodium pyrophosphate, 0.1mM sodium orthovanadate, 2µM microcystin LR, 1mM benzamidine) by passing them 10 times through a 22-gauge needle. Lysates were centrifuged at 800 x g for 5 min at 4°C. The nucleus pellet was solubilized in Buffer B (400mM NaCl, 2mM Na<sub>3</sub>VO<sub>4</sub>, 1mM EGTA, 1mM DTT) while supernatants were further centrifuged at 100,000 x g for 20 min at 4°C. The final supernatants represents the cytosolic fraction. The membrane pellet was solubilized in Buffer A containing 1% Triton X-100 and further centrifuged at 12,000 x g for 10 min at 4°C.

### **3.8 Measurement of Rho activity**

Cellular Rho activity was measured by pull down assay using the Rho binding domain of Rhotekin fused to GST (GST-RBD). For determining Rho activity cells were extracted in Tris buffer (1% Triton X-100, 150 mM NaCl, 10 mM MgCl<sub>2</sub>, 10 mg/ml leupeptin, 10 mg/ml aprotinin, 1 mM PMSF). Rho activity (percentage of GTP-bound Rho) is determined as the amount of RBD-bound Rho versus the total Rho in the lysate (Vial et al. 2003).

### **3.9 Scratch wound healing assay**

Endothelial cells and fibroblasts were seeded at a density of  $8 \times 10^5$  cells per well into the uncoated 6-well microplates, wounded by manually scratching with a pipette tip, washed twice with phosphate-buffered saline (PBS) and incubated at 37°C, with or without mitomycin C (10 µg/ml), PD98059 (30 µM) or BDM (5 µM), as indicated in individual experiments. Wound gap was photographed at 0 and 24 h at the same location. Images of areas were collected with a camera coupled to the microscope and percentage of closure was calculated with NIH IMAGE J. These experiments were repeated at least three times.

### **3.10 Time-Lapse Microscopy**

Time-lapse microscopy (TLM) experiments were performed by using a video optical microscopy workstation which has been already described elsewhere

(Dickinson and Tranquillo 1993). The images are captured by a cooled monochromatic CCD video camera. The samples were imaged every 10 min with a long working distance 10x objective in phase contrast for overall 24 h. The scratch assay were carried out in the TLM experiments and cell motion was analyzed offline as described in the following.

### 3.11 Cell Tracking

Image analysis of the scratch assay was performed by using a semi-automated Cell Tracking software. For each time step, about 40 cells on the wound edges were individually followed by manual overlaying each cell contour, and the coordinates of the contour points and of the cell centre of mass are stored on hard disk. To assist the operator in cell identification, the color-coded contour of each cell at the previous time step is also shown in the image overlay. From the centre of mass coordinates the trajectory of each cell was reconstructed for the whole experiment. Furthermore, average motility parameters of the cell population, such as velocity, were calculated as a function of time. The analysis of cell motility was based on the persistent random walk theory (Dickinson et al 1994; Matthes et al 1998), where it is assumed that cell motion is characterized by a diffusion coefficient (also referred to as the random motility coefficient)  $D$  ( $\mu\text{m}^2/\text{min}$ ) and a persistent time  $P$  (min). According to the theory, the mean square displacements are given by the equation

$$\langle d^2(t) \rangle = 4D \left[ t - P(1 - e^{-t/P}) \right] \quad (1)$$

where  $\langle d^2(t) \rangle$  ( $\mu\text{m}^2$ ) is the mean square displacement of the tracked cell sample at time  $t$ . The trend predicted by Eq. 1 is linear at  $t \gg P$  (i.e.,  $\langle d^2(t) \rangle \approx 4Dt$ ), with a slope proportional to the diffusion coefficient. The mean square displacements are calculated from the following relation

$$\langle d^2(k) \rangle = \sum_{i=1}^N \sum_{j=1}^{M-k} \left[ (x_i(j+k) - x_i(j))^2 + (y_i(j+k) - y_i(j))^2 \right] \quad (2)$$

where  $k$  is the current time expressed in units of the time interval  $\mu t$  between two consecutive image acquisitions, the double summation is on the index  $i$  representing cell number (up to the total cell number  $N$ ) and on index  $j$  representing the number of intervals (the total number being  $M-k$ ),  $x$  and  $y$  are the centre of mass coordinates obtained by cell tracking. The mean square displacements are calculated from non-overlapping intervals (Dickinson et al 1994). Eq. (1) was fit to the experimental data of mean square displacements

(calculated from Eq. (2)) as a function of time with  $D$  and  $P$  as the only adjustable parameters.

### **3.12 Cytoplasmic spreading**

Fibroblasts were seeded at a density of  $1 \times 10^4$  cells per well into the 12-well microplates coated with fibronectin (1  $\mu\text{g}/\text{well}$ ) or heat-denatured BSA, as a negative control. Then after 3 h, cells were gently washed with PBS and fixed in 4% formaldehyde for 15 min. After staining with 0.1% crystal violet, the cells were examined by microscopy. Five randomly chosen visual fields, representing approximately 15% of the dish surface area, were photographed and the number of cells was counted (at least 1000 cells). The cells were scored as either non-spreaded or spreaded (cells that had become flattened with their total diameter more than twice the diameter of the nucleus) (Enserink et al. 2004).

### **3.13 Confocal microscopy**

Subconfluent cells on glass coverslips were fixed for 20 min with 4% paraformaldehyde (Sigma) in PBS containing 0.9mM calcium and 0.5mM magnesium (PBS CM) at room temperature, washed twice in 50mM  $\text{NH}_4\text{Cl}$  in PBS CM and twice in PBS CM. Cells were permeabilized for 5 min in 0.5% Triton-X 100 (Bio-Rad) in PBS CM, washed twice, for 10 min, in 0.2% gelatin (Sigma) in PBS CM and then incubated for 1 h with the primary antibodies diluted in 0.5% BSA (Sigma) in PBS. After three washes with 0.2% gelatine, cells were incubated for 20 min with the appropriate rhodamine- or fluorescein-tagged goat anti-mouse or anti-rabbit secondary antibody (Jackson ImmunoResearch, West Grove, PA), diluted 1:50 in 0.5% BSA in PBS. After final washes with PBS, the coverslips were mounted on a microscope slide using a 50% solution of glycerol in PBS and examined with a Zeiss LSM 510 version 2.8 SP1 Confocal System. The experiments were done with or without treatment with 30  $\mu\text{M}$  PD98059.

## 4. RESULTS AND DISCUSSION

### 4.1 *Ped/Pea-15* effect on wound healing *in vivo*.

In order to assess the role of *Ped/Pea-15* during skin wound healing, full thickness wounds were performed on the back of TgPED and Wt mice and several wound healing parameters were evaluated to follow the repair process. At 4 days after a dorsal incision, the distance between the wound edges was about 3-fold higher in TgPED mice compared to their respective Wt littermates (Table 1). Also, after 6 days, a complete closure of the wound was observed in all Wt while not in TgPED mice (data not shown). TgPED mice also presented significantly reduced granulation tissue formation as compared to Wt (Table 1). Histological exam of the wounded skin revealed a significant reduction in the skin fibroblasts content and a comparable reduction of collagen fibres in the PEDTg specimens, compared to those observed in the Wt. Wounded skin of TgPED mice also exhibited an increased detection of infiltrated inflammatory cells which probably contributes to the inhibition of healing progression (Table 1).

Table 1: Assessment of wound healing parameters in Wt and TgPED mice 3 days post-wounding.

Genotype	Epidermal closure (mm)	Granulation tissue thickness (%)	Collagen fibres production	Activated fibroblasts content	Infiltrated cells content
Wt	0.6±0.6	70	1.4±0.7	1.6±1	1±0.9
TgPED	1.7±1.4 (p<0.001)	40 (p<0.001)	0.6±0.9 (p<0.001)	0.9±1 (p<0.01)	1.5±1.3 (p<0.01)

### 4.2 *In vivo* evaluation of mice inflammatory state

The first stage of the wound healing process is the inflammatory response to the hurt damage and the inflammatory cytokines produced at this moment are important to sustain the tissue repair (Acosta et al 2008). Then, to understand if *Ped/Pea-15* overexpression contributes to the impaired wound healing observed in TgPED mice since the first stage of the repair process, plasma levels of several inflammatory cytokines were measured at 24 h after the dorsal incision of mice. Between the cytokines detected, IL-6, Eotaxin, INF- $\gamma$ , MCP-1, MIP-1 $\alpha$ , MIP-1 $\beta$ , TNF- $\alpha$  were increased in the plasma of TgPED mice compared to Wt littermates,

while the concentration of IL-12 results reduced (Table 2). This altered inflammatory state was in agreement with the increased infiltrated inflammatory cells observed in the skin biopsies of TgPED mice and may contribute at least in part to the reduced granulation tissue, collagen fibres production and reduced fibroblast content detected in the skin specimen.

**Table 2: Assessment of cytokine expression in Wt and TgPED mice 3 days post-wounding.**

Genotype	Eotaxin (pg/ml)	IL-6 (pg/ml)	INF- $\gamma$ (pg/ml)	MCP-1 (pg/ml)	TNF- $\alpha$ (pg/ml)	IL-12 (pg/ml)	MIP1- $\alpha$ (pg/ml)	MIP1- $\beta$ (pg/ml)
Wt	918	64	110	382	2222	222	299	194
TgPED	1554 (p<0.05)	424 (p<0.05)	160 (p<0.05)	657 (p<0.01)	3214 (p<0.01)	90 (p<0.05)	728 (p<0.05)	445 (p<0.05)

#### 4.3 Assessment of angiogenic response in mice skin

The aim of this experiment was to replicate the angiogenic response that occurs in the wound healing process. In these pathological conditions angiogenesis develops in response to an imbalance of positive and negative effectors that result in a gradient of positive angiogenic stimuli, with the direction of initial endothelial sprouting occurring along the axis of this gradient (Galkowska 2006). We used the angioreactor containing a reconstituted extracellular matrix enriched or not with pro-angiogenic factors to stimulate a neo-angiogenic response. Angioreactors were implanted in the back of each mouse. At 9 days after implantation, angioreactors were dissected from Wt and TgPED mice and visually inspected for angiogenesis. For both Wt and TgPED mice the angiogenic response was observed only in the FGF -2/VEGF-containing angioreactors. However, the extent of this response was significantly reduced in TgPED mice compared to controls (Figure 5).

#### 4.4 Effect of *Ped/Pea-15* on endothelial cells migration and tube formation

Angiogenesis, the biological process leading to the formation of new blood vessels, is a process including endothelial cells (EC) proliferation, migration and formation of new capillaries (Hanahan and Folkman 1996). In order to better clarify the angiogenic response in mice overexpressing *Ped/Pea-15*, endothelial

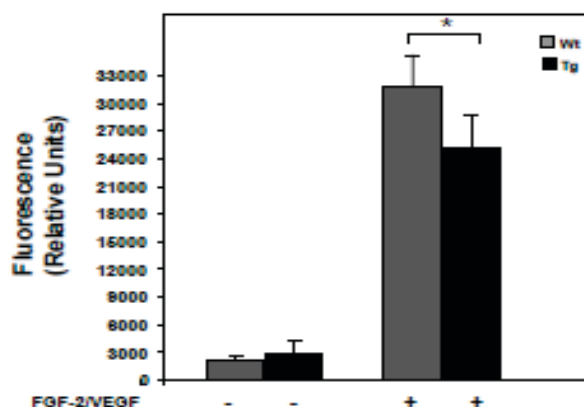


**Figure 5. Quantification of DIVAA by FITC-dextran injection and validation of endothelial responses.** Angioreactors are prepared and surgically implanted in mice as described in Materials and Methods. At 9 day after implantation, responses in both FGF-2 and VEGF (500 ng/ml) containing Matrigel and Matrigel without angiogenic factors, as indicated, are determined by fluorescence quantitation of FITC-dextran. Results are expressed as relative fluorescence units of FITC-dextran. Results of three independent experiments were shown. Asterisks denote statistically significant differences (\* $p < 0.05$ ).

cells from TgPED and Wt mice were isolated. Cells were subjected to scratch wound healing assay and to matrigel assay to measure cell migration and tube formation ability respectively. Our results showed that TgPED EC have an impaired migration ability compared to those isolated from Wt mice (Figure 6). Furthermore matrigel assays indicated also a reduction in the capillary-like tube formation than those of Wt EC (Figure 7).

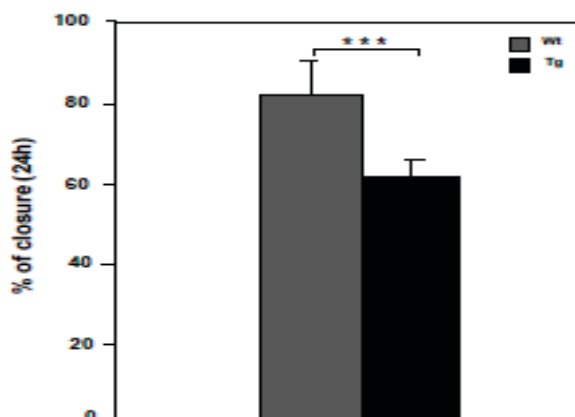


**Figure 6. Wound healing in cultured endothelial cells from TgPED mice.**

Confluent monolayers of endothelial cells from Wt and TgPED mice were subjected to scratch wound healing assays, as described in Materials and Methods. Healing was calculated as described in Materials and Methods. Bars represent the means  $\pm$  SD of triplicate determination in four independent experiments. Asterisks denote statistically significant differences (\*\* $p < 0.001$ ).

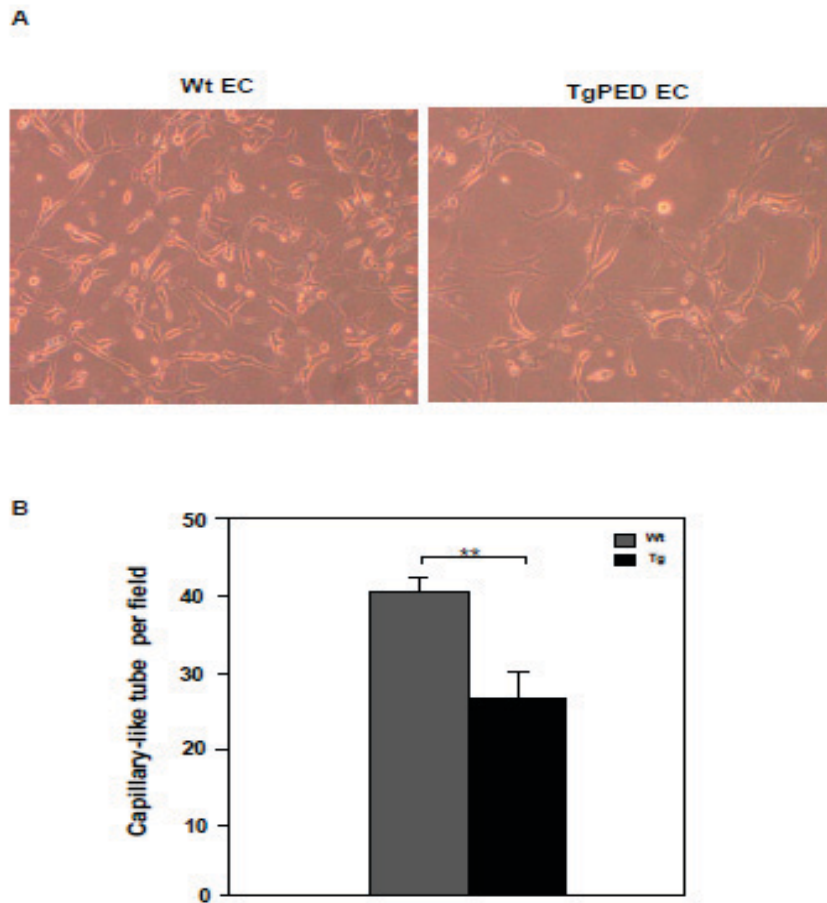


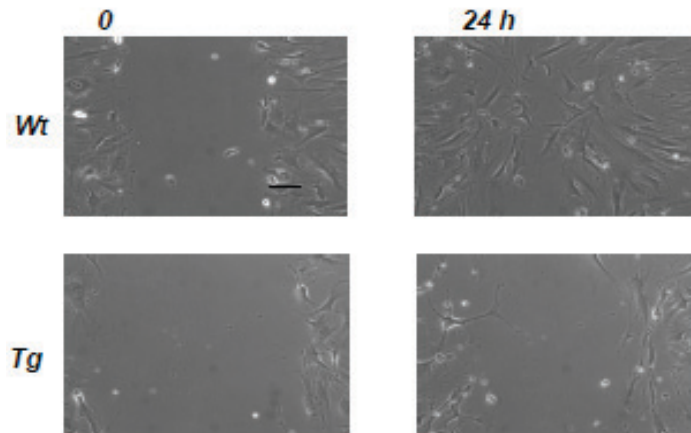
**Figure 7. Capillary-like tube formation of endothelial cells isolated from TgPED and Wt mice.** A) Representative images of capillary-like tube formation in endothelial cells from TgPED and Wt mice on Matrigel after 8 days of culture. B) Statistical analysis of tube formation by counting all branches in three randomly chosen fields from each well. The experiment was repeated three times. Asterisks denote statistically significant differences (\*\* $p < 0.01$ ).

#### 4.5 Effect of Ped/Pea-15 on fibroblasts involved in the wound healing

The components of the granulation tissue include fibroblasts, collagen (produced by fibroblasts) and blood vessels. In the wound healing process, fibroblasts produce the collagen-based ECM and help the reapproximate of the wound edges through their contractile properties (Lawrence 1998). We study the wound closure in skin fibroblasts isolated from TgPED mice and in their Wt littermates. Confluent monolayers of cells were scratched and images were taken at 0 and 24 hours after wounding (Figure 8A). The wound closure was significantly decreased in TgPED fibroblasts compared to controls (Fig. 8B). To determine whether the effect of ped/pea-15 was due to alteration of cell proliferation, scratch wound

healing assays were also performed in the presence of 10  $\mu\text{g/ml}$  mitomycin C, an irreversible inhibitor of mitosis. Treatment with mitomycin C decreased the wound closure rate in fibroblasts of both genotypes. However, the extent of closure of TgPED fibroblasts was still reduced compared to controls (Figure 8B).

....A



B

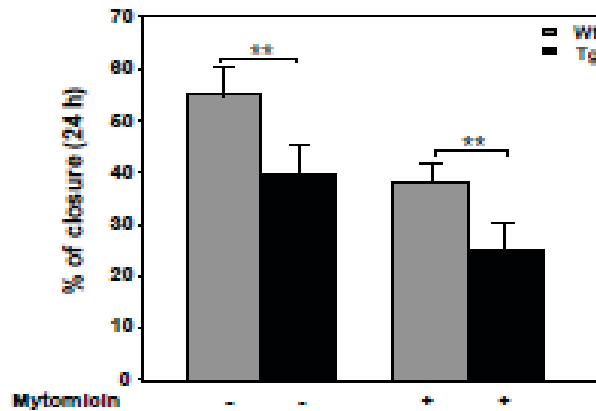


**Figure 8. Wound healing in cultured fibroblasts from TgPED mice.**

A) Confluent monolayers of fibroblasts from Wt and TgPED mice were subjected to scratch wound healing assays, as described in Materials and Methods. Phase contrast microscopy images of cultured fibroblasts from TgPED mice and their Wt controls. B) Scratch assays were performed in the absence or in the presence of 10  $\mu\text{g/ml}$  Mitomycin C, as indicated. Healing was calculated as described in Materials and Methods. Bars represent the means  $\pm$  SD of triplicate determination in four independent experiments. Asterisks denote statistically significant differences (\*\* $p < 0.01$ ).

Moreover, no difference between Wt and TgPED fibroblasts was detected in thymidine incorporation experiments (data not shown), suggesting that ped/pea-15 effect on wound closure was not due to changes in cell proliferation.

#### 4.6 Direct evaluation of fibroblast motility by time-lapse microscopy (TLM)

Fibroblast motility was then assessed by quantitative analysis of images acquired in TLM experiments (see Materials and Methods) following the scratch and images were recorded with a time interval of 10 min for 24 h. Wound closure was visually almost complete in 24 h for Wt cells, whereas TgPED fibroblasts were lagging behind. In agreement with the striking difference in wound closure rate, TgPED fibroblasts exhibited a significantly lower average velocity (Table 3). Moreover, cell trajectories were reconstructed by the cell tracking image analysis (see Materials and Methods). In both Wt (Fig. 10A) and TgPED (Fig. 10B) fibroblasts, the trajectories showed a random orientation being uniformly distributed in space (i.e., no preferential direction of motion can be distinguished). However, more extended cell trajectories were detected in Wt compared to TgPED fibroblasts (Fig. 10A-B). The mean square displacements  $\langle d^2(t) \rangle$  of the two populations were calculated from the cell centers of mass at each time (see Eq. 2 in Materials and Methods). The  $\langle d^2(t) \rangle$  values, which are representative of cell migration by random diffusion, were about 2-fold higher in Wt fibroblasts. Accordingly, the values of D (diffusion coefficient) and P (persistence time) were about 2-fold higher in Wt compared to TgPED fibroblasts (Table 3).

Table3: Assessment of motility parameters in fibroblasts from Wt and TgPED mice

Genotype	Velocity ( $\mu\text{m}/\text{min}$ )	D ( $\mu\text{m}^2/\text{min}$ )	P (min)
Wt	0.9 $\pm$ 0.08	8.3 $\pm$ 2.7	332 $\pm$ 75
TgPED	0.5 $\pm$ 0.09 (p<0.01)	3.9 $\pm$ 1.2 (p<0.01)	143 $\pm$ 25 (p<0.01)

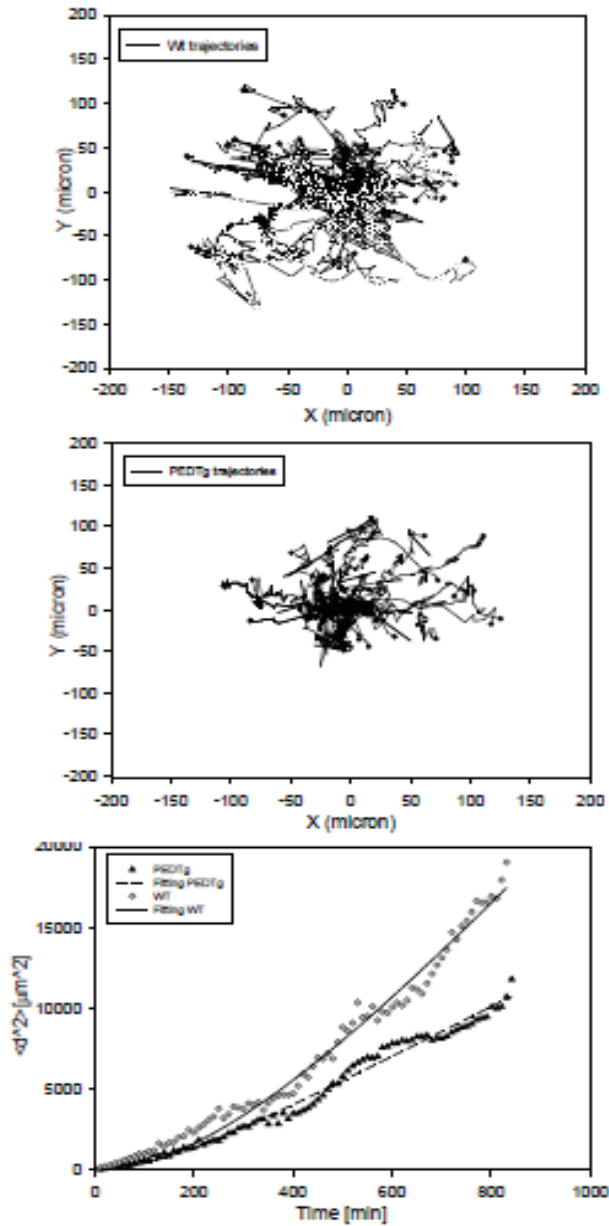


**Figure 9. Fibroblast trajectory analysis and mean square displacements.** A direct analysis of cell trajectories is used to characterize the motion of Wt (A) and TgPED fibroblasts (B). The trajectory of each cell is represented by the sequence of the cell centre of mass positions translated to start from the same origin. To quantitatively assess cell movement, the mean square displacements (C) are calculated for a population of 40 cells tracked for 16 h by using Manual Cell Tracking as described in Experimental procedures

#### 4.7 Ped/Pea-15 effect on cell adhesion, spreading and cytoskeleton organization

Fibroblast motility is dependent on cell ability to adhere to substrate and to transfer into the cytoplasm the signal that induces the cytoskeleton reorganization (Ridley et al 2003; Arnaout et al 2007). TgPED fibroblasts showed no significant difference in adhesion compared to the controls (data not shown). Moreover, after 3 h plating on fibronectin, about 60% of Wt cells exhibited a spread cytoplasm. By contrast, the number of spread cells was about 30% for TgPED (Figure 10).

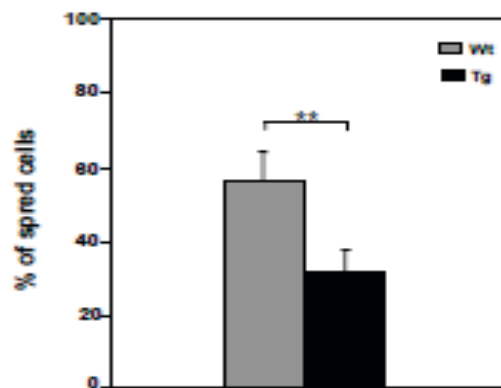


**Figure 10. Cytoplasmic spreading in Wt and TgPED fibroblasts.** Fibroblasts from Wt and TgPED mice were subjected to spreading assays. After 3h plating on fibronectin, cytoplasmic spreading was quantified by light microscope after staining with crystal violet as described in Materials and Methods. Bars represent the means  $\pm$  SD of three independent determinations in triplicate. Asterisks denote statistically significant differences (\*\* $p < 0.01$ )

To analyze actin cytoskeleton and focal adhesion plaques organization, Wt and TgPED fibroblasts were stained with rhodamin-conjugated phalloidin or with specific anti-paxillin antibodies, respectively. Clearly, the results showed that at least 70% of TgPED fibroblasts displayed a marked decrease of stress fibres and focal adhesion plaques compared to controls (Figure 11).

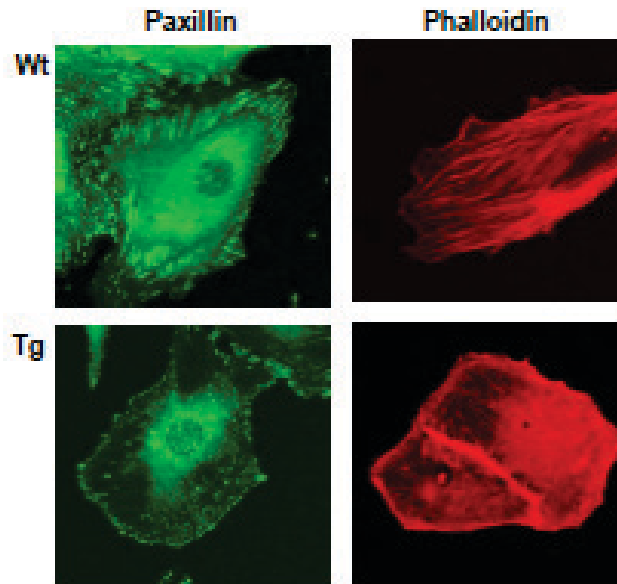


**Figure 11. Cytoskeleton organization in Wt and TgPED fibroblasts.** Immunofluorescence analysis was performed as described in Materials and Methods. Focal adhesion plaques formation were investigated by immunostaining with specific anti-paxillin antibody. Stress fibers organization were detected by rhodamine-phalloidin staining. The experiment was repeated four times with similar results. A sample image is shown.

#### **4.8 *Ped/Pea-15* effect on RhoA activity and subcellular distribution.**

RhoA-GTPase is a protein that plays a major role in stress fibres organization and focal adhesion plaque formation in the cytoplasm (Huvemners et al 2009). When released from Rho GDP dissociation inhibitors (GDIs), Rho-GTPases are targeted to the plasma membrane, where its activation cycle is regulated by guanine-exchange factors (GEFs) that promote GTP loading and activation of Rho-GTPases (Raftopoulou et al 2004). RhoA activity was assessed in pull down assay by measurement of the levels of active GTP bound protein. In TgPED fibroblasts the levels of active RhoA were decreased with no change in RhoA expression compared to Wt cells (Figure 12A). Moreover, RhoA membrane localization was markedly decreased in TgPED fibroblasts compared to control cells (Figure 12B). Consistently, RhoA cytosolic detection was much stronger in TgPED than in Wt fibroblasts, suggesting an aberrant localization of the protein.

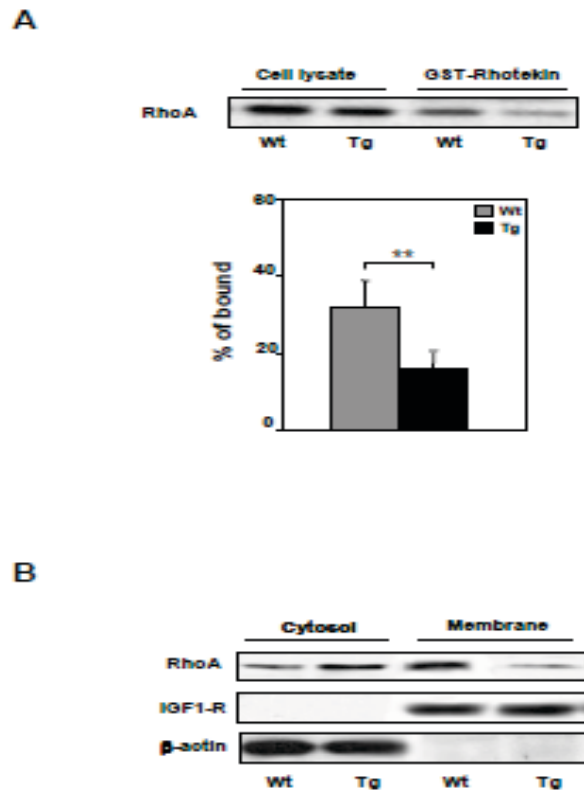


**Figure 12. RhoA activity and localization in fibroblasts from Wt and TgPed fibroblasts.** A) Cell lysates were obtained from Wt and TgPED fibroblasts as described in Materials and Methods. Pull-down assays with GST-Rhotekin were performed and analyzed by Western Blot. Densitometry for pulled-down RhoA-GTP was normalized to the amount of total RhoA. The results are presented as percentage of bound respect to total level of protein. Data are mean of four independent experiments. Asterisks denote statistically significant differences (\*\* $p < 0.01$ ). B) Cytosolic and membrane fractions of Wt and TgPED fibroblasts were obtained as described in Materials and Methods. Western blot with anti-RhoA,  $\beta$ -actin and IGF-1 receptor  $\beta$ -subunit antibodies was performed. Autoradiographs representative of four independent experiments are shown.

#### 4.9 *Ped/Pea-15* effect on ERK 1/2 activation and function in wound healing alteration

It has been previously demonstrated that *ped/pea-15* increased activation of ERK1/2 in CHO cells (Ramos et al. 2000). We have therefore tested ERK1/2 phosphorylation in Wt and TgPED fibroblasts. As expected, ERK1/2 activation was increased in TgPED fibroblasts compared with Wt fibroblasts (Figure 13A).

Moreover ped/pea-15 overexpression increased ERK1/2 cytosolic localization in TgPED fibroblasts compared to the control cells (Figure 13B).

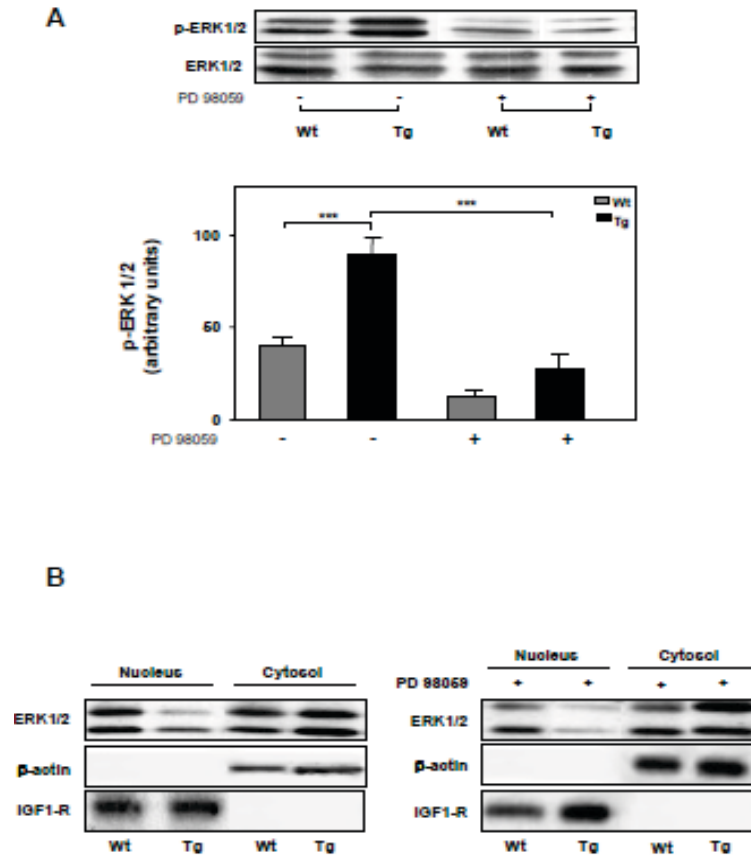


**Figure 13. Evaluation of ERK 1/2 activation by PED/PEA-15 in Wt and TgPED fibroblasts.** A) Cells were treated with PD98059 as described in Materials and Methods and solubilized. Western blot with with anti-phospho-ERK1/2 and ERK1/2 antibodies was performed and autoradiographs were subjected to densitometric analysis. B) Cytosolic and membrane fractions of Wt and TgPED fibroblasts were obtained in the absence or in the presence of 30  $\mu$ M PD98059, as described in Materials and Methods. Western blot with anti-ERK1/2,  $\beta$ -actin and IGF-1 receptor  $\beta$ -subunit antibodies was performed. All the blots shown are representative of four independent experiments.

To assess whether ERK1/2 hyperactivation could be responsible for wound closure and spreading alterations as well as for the decreased RhoA activation, rearrangement of RhoA localization and organization of cytoskeleton structures, fibroblasts from both Wt and TgPED mice were treated with 30  $\mu$ M PD98059 (an inhibitor of the MEK-ERK1/2 pathway). At this concentration PD98059 did not affect both proliferation and morphology of Wt and TgPED fibroblasts (data not

shown), as well as ERK1/2 localization (Figure 13B). Nevertheless it was able to reduce ERK 1/2 phosphorylation in both cellular types (Figure 13A). Treatment with PD98059 increased wound closure in Wt fibroblasts and almost completely rescued wound closure in TgPED fibroblasts (Figure 14).

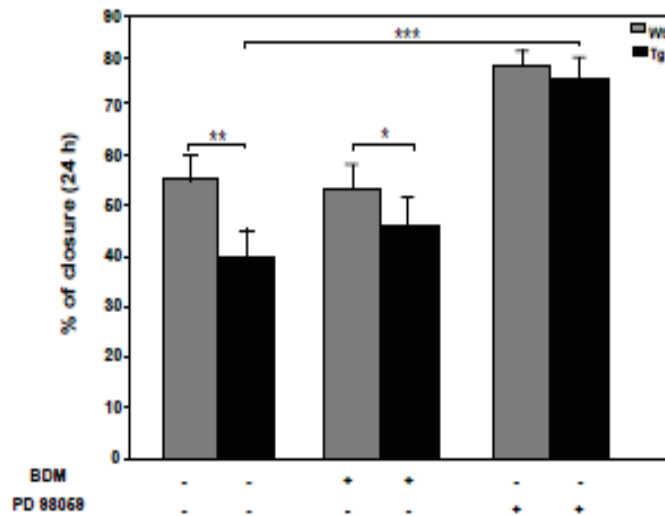


**Figure 14. Effect of PKC and ERK inhibitors on *in vitro* wound healing.** Confluent monolayers of fibroblasts from Wt and TgPED mice were subjected to scratch assays, as described in Materials and Methods. The scratch assays were performed in culture medium alone or added with 5  $\mu$ M BDM or 30  $\mu$ M PD98059, as indicated. Healing was calculated as described in Materials and Methods. Bars represent the means  $\pm$  SD of triplicate determination in four independent experiments. Asterisks denote statistically significant differences (\* $p$ <0.05; \*\* $p$ <0.01; \*\*\* $p$ <0.001).

At variance, in both Wt and TgPED fibroblasts, almost no effect was elicited by treatment with 5  $\mu$ M bisindolylmaleimide (BDM), which inhibited PKC activity in both cell type (data not shown). Moreover, treatment with PD98059 completely reverted the effect of PED/PEA-15 on spreading (Figure 15A) and determined a substantial rescue of stress fibres and focal adhesion plaques in about 90% of TgPED fibroblasts, compared to the controls (Figure 15B). Similarly, PD98059 treatment restored RhoA activity (data not shown) and plasma membrane content in TgPED fibroblasts to the levels observed for Wt fibroblasts (Fig. 15C).

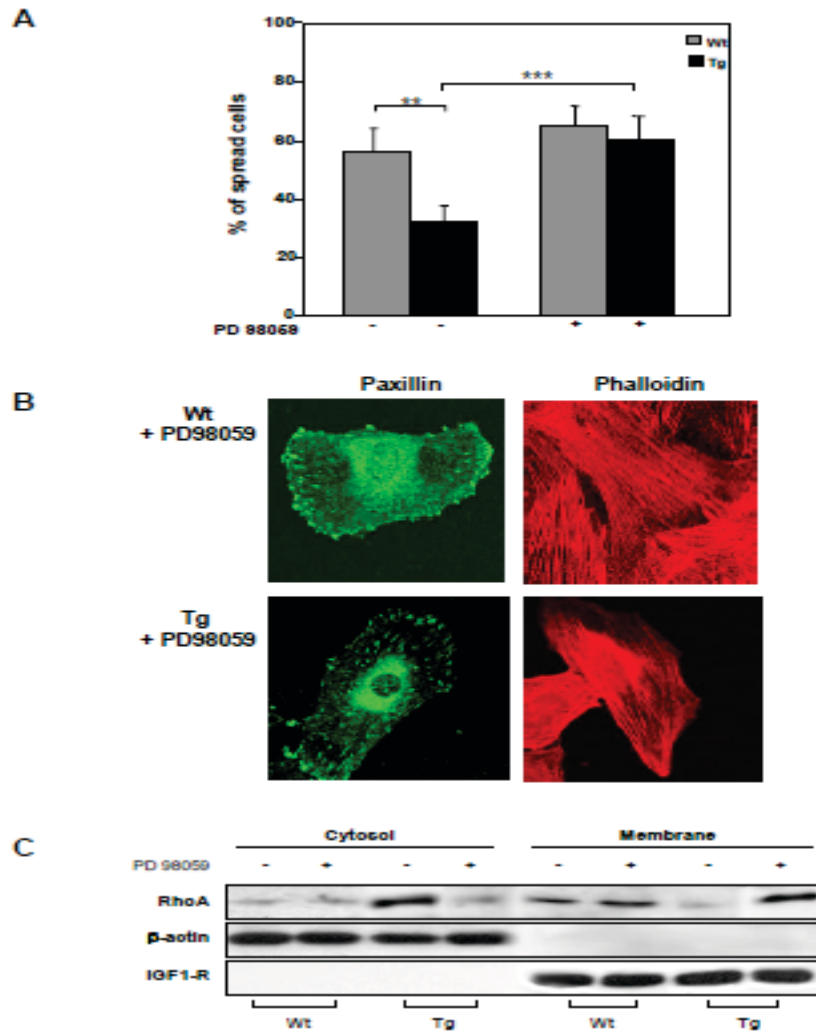


**Figure 15. Effect of PD98059 on spreading, cytoskeleton organization and RhoA localization.**

A) Cytoplasmic spreading was quantified in TgPED fibroblasts pre-incubated in the absence or in the presence of 30  $\mu$ M PD98059, as indicated, as described in Materials and Methods. Bars represent the means  $\pm$  SD of three independent determinations in triplicate. Asterisks denote statistically significant differences (\*\* $p < 0.01$ ; \*\*\* $p < 0.001$ ). B) Immunofluorescence analysis was performed in Wt and TgPED fibroblasts incubated with 30  $\mu$ M PD98059. Focal adhesion plaques formation was investigated by immunostaining with specific anti-paxillin antibody. Stress fibers were detected by rhodamine-phalloidin staining. The experiment was repeated four times with similar results. A sample image is shown. C) Cytosolic and membrane fractions of Wt and TgPED fibroblasts cultured in the absence or in the presence of 30  $\mu$ M PD98059, as indicated, were obtained as described in Materials and Methods, subjected to SDS-PAGE and immunoblotted with anti-RhoA,  $\beta$ -actin and IGF-1 receptor  $\beta$ -subunit antibodies. Blots were revealed by ECL and autoradiography. The blots shown are representative of four independent experiments

#### 4.10 Ped/Pea-15 depletion increased fibroblast spreading and wound closure

To further address the role of *ped/pea-15* in the regulation of cellular motility, we used fibroblasts from *ped/pea-15* null mice (KO). These animals have been previously characterized and reported (Miele et al. 2007) and feature no PED/PEA-15 expression in skin fibroblasts (data not shown). Importantly, after 3 h plating on fibronectin, cytoplasmic spreading was increased by about 30% compared to control cells (Figure 16A). Likewise, the ability to recolonize the wounded area was also increased in *ped/pea-15* null fibroblasts (Figure 16B). Furthermore, wound closure was almost complete after 16 h in KO fibroblasts, while it occurred at least after 24 h in control mice.

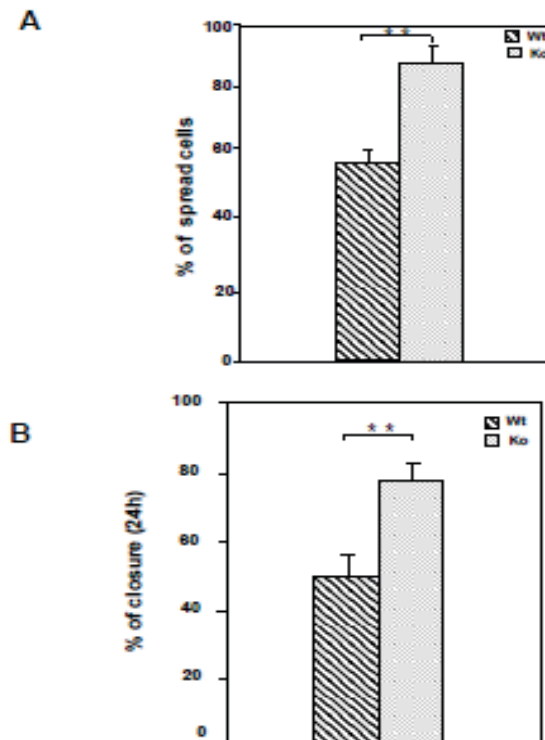


**Figure 16. Cytoplasmic spreading and *in vitro* wound healing in *ped/pea-15* null fibroblasts.** A) Fibroblasts from Wt and *ped/pea-15* null mice were subjected to spreading assays. After 3h, cytoplasmic spreading on fibronectin was quantified by light microscope after staining with crystal violet as described in Experimental procedures. Bars represent the means  $\pm$  SD of three independent determinations in triplicate. Asterisks denote statistically significant differences (\*\* $p < 0,01$ ). B) Confluent monolayers of fibroblasts from Wt and *ped/pea-15* null mice were subjected to scratch assays, as described in Materials and Methods. Healing was calculated as described in Experimental procedures. Bars represent the means  $\pm$  SD of triplicate determination in four independent experiments. Asterisks denote statistically significant differences (\*\* $p < 0.01$ ).

Finally we have also examined wound healing in KO mice. In these mice the distance between the wound edges was about 2-fold lower compared to their respective Wt littermates. Moreover, the content of activated fibroblasts was significantly increased in KO mice (Table 3).

Table 3: Assessment of wound healing in KO mice 4 days post-wounding.

<b>Genotype</b>	<b>Epidermal closure (mm)</b>	<b>Activated fibroblasts content</b>
<b>Wt</b>	0.8±0.2	1.4±1
<b>KO</b>	0.4±0.1 (p<0.05)	1.9±0.3 (p<0.05)

## 5. CONCLUSIONS

Transgenic mice overexpressing *PED/PEA-15* (TgPED) to levels comparable to those occurring in patients with type 2 diabetes, display altered glucose tolerance and impaired insulin secretion. Here, we show that TgPED mice display also an impaired skin wound healing when subjected to dorsal incision and that their phenotype reflects, at least in part, the phenotype of chronic non-healing ulcers of diabetic patients.

The analysis of all stages revealed that the process of skin wound healing is altered in each phase in the TgPED mouse model: inflammation, granulation tissue formation and re-epithelization. Similar as the human pathological ulcers, the repair process which occurs after injury is stalled in the inflammatory phase. This is confirmed by the increased infiltrate of inflammatory cells in the TgPED mice skin specimens and by the increase in the serum concentration of some inflammatory cytokines. Persistently high levels of TNF- $\alpha$  and related cytokines as IL-6, Eotaxin, INF- $\gamma$ , MCP-1, MIP1- $\alpha$  and MIP1- $\beta$  adversely affect the growth, the viability and the functions of cell types necessary for appropriate formation of a healthy extracellular matrix, such as endothelial cells and fibroblasts (Acosta et al. 2008). Indeed in TgPED mice we found a decreased growth of the granulation tissue, a tissue that come from endothelial cells and fibroblasts migration and proliferation in the wound bed. Moreover we found a reduced capillary tube formation, a reduction in fibroblasts content and a collagen fibres production. Thus, likewise diabetic patients, TgPED mice have impaired fibroblast migration and insufficient angiogenesis to support the collagen synthesis necessary for mature granulation and subsequent re-epithelialization (Falanga 2005). Then, in TgPED mice the altered wound healing may be due to the high levels of inflammatory cytokines and in particular TNF- $\alpha$ . This is consistent with recent observation indicating that low concentrations of TNF- $\alpha$  stimulate fibroblasts to repopulate a wound space, enhance collagen production, promote angiogenesis, accelerate reepithelialization with significantly less neutrophil and macrophage infiltration, and decrease gene expression of several inflammatory molecules, while at high levels of TNF- $\alpha$  all these processes are impeded (Berrientos et al. 2008; Weinstein and Kirsner 2010). Then we focused our attention on the study of endothelial cells and fibroblasts isolated from TgPED and Wt mice. Both cells type showed a migratory defect. This is in agreement with the results obtained with the in vivo studies. It should be noticed that TgPED mice displayed reduced glucose tolerance and impaired insulin sensitivity (Vigliotta et al. 2004). Thus it is possible that metabolic abnormalities may confer to the isolated cells, phenotypes reminiscent of the “in vivo” metabolic milieu. Indeed metabolic memory is generally recognized to participate to the pathogenesis of diabetes and its complications

(Villeneuve and Natarajan 2010). However, cells isolated from TgPED mice live for several generations in culture, independently of the metabolic status, raising the possibility that PED/PEA-15 may directly regulate the motility phenotype. In support of this latter hypothesis, it should be mentioned that cells in which PED/PEA-15 cDNA has been overexpressed display defects in cellular adhesion and integrin signalling (Krueger et al 2005). Furthermore we have also demonstrated that in scratch wound healing assay, closure was accelerated in fibroblasts isolated from *ped/pea-15* null mice.

Collectively, these data suggest that PED/PEA-15 is able to impair skin wound healing, in particular modulating the functions of cells that are involved in the repair process, and open the way for future investigations on its role in diabetic complications.

## 6. ACKNOWLEDGMENTS

*Vorrei ringraziare:*

*Prof. F. Beguinot, per avermi dato la possibilità di essere parte del suo laboratorio di ricerca, e per essere esempio di costante dedizione al lavoro.*

*Prof. P. Formisano e la Dott.ssa Claudia Miele, per essere stati una guida in questi anni e per i continui suggerimenti scientifici.*

*Dr.ssa Angela Cassese e Dr.ssa Ginevra Botta. “ In questi anni ho ritrovato in voi due amiche sincere ed affettuose, grazie per aver condiviso con me tanti momenti della mia vita e per essere state sempre un valido appoggio soprattutto nei momenti difficili”*

*Dr.ssa Claudia Iadicicco, Dr.ssa Cecilia Nigro, Dr.ssa Annalisa Ilardi, Dr.ssa Angela Lombardi, e il Dr. Michele Longo per aver reso allegre e serene tutte le giornate trascorse insieme in laboratorio*

*Dr. Giuseppe Perruolo, Dr.ssa Serena Cabaro, Dott.ssa Francesca Fiory, Dr. Francesco Oriente e tutto il DiabLab.....è stato un piacere lavorare con voi in questi anni!!!*

*Mio marito Ivan, per essere stato il mio vero pilastro in questi anni, per aver creduto in me e aver sostenuto sempre con amore incondizionato e fiducia ogni mia decisione.*

## 7. REFERENCES

- Acosta JB, del Barco DG, Vera DC, Savigne W, Lopez-Saura P, Nieto GG, Schultz GS. The pro-inflammatory environment in recalcitrant diabetic foot wounds. *Int Wound J* 2008; 5:530–539
- Alberts B, Johnson A, Lewis J, Raff M, Roberts K, Walter P. *Molecular Biology of the Cell*. Fourth Edition.
- Altshuler D, et al. The common PPAR $\gamma$  Pro12Ala polymorphism is associated with decreased risk of type 2 diabetes. *Nature Genet.* 2000; 26:76-80.
- Arnaout MA, Goodman SL, Xiong JP. Structure and mechanics of integrin-based cell adhesion. *Curr Opin Cell Biol* 2007; 19:495-507
- Atala A, Lanza RP. *Methods of tissue engineering*. Academic Press, London, UK 2001.
- Avruch A, Khokhlatchev J, Kyriakis M, Luo Z, Tzivion G, Vavvas D, Zhang XD. Ras activation of the Raf kinase: tyrosine kinase recruitment of the MAP kinase cascade. *Recent Progress in Hormone Research* 2001; 56:127-155
- Baum CL, Christopher J. Normal cutaneous wound healing: clinical correlation with cellular and molecular events. *Dermatol Surg.* 2005; 31: 674-686
- Berrientos S, Stojadinovic O, Golinko M, BremH, Tomic-Canic M. Growth factor and Cytokine in wound healing. *Wound Rep Reg* 2008;16:585-601
- Blumberg, M.P. Protein kinase C and signal trasduction in normal and neoplastic cells. *Cellular and molecular pathogenesis* 1996; 389-402.
- Braiman-Wiksman L, Solomonik I, Spira R, Tennenbaum T. Novel insights into wound healing sequence of events. *Toxicologic Pathology* 2007; 35: 767-779
- Borst SE. The role of TNF-alpha in insulin resistance. *Endocrine* 2004;23:177–82
- Calhoun JH, Overgaard KA, Stevens CM, Dowling JP, Mader JT. Diabetic foot ulcers and infections: current concepts. *Adv Skin Wound Care* 2002; 15:31-45
- Cantrell D. Phosphoinositide 3-kinase signalling pathways. *J Cell Sci.* 2001;114:1439-1445.

Condorelli G, Vigliotta G, Iavarone C, Caruso M, Tocchetti CG, Andreozzi F, Cafieri A, Tecce MF, Formisano P, Beguinot L, Beguinot F. PED/PEA-15 gene controls glucose transport and is overexpressed in type 2 diabetes mellitus. *EMBO J.* 1998; 17(14):3858-66.

Condorelli G, Vigliotta G, Trencia A, Maitan MA, Caruso M, Miele C, Oriente F, Santopietro S, Formisano P, Beguinot F. Protein kinase C (PKC)-alpha activation inhibits PKC-zeta and mediates the action of PED/PEA-15 on glucose transport in the L6 skeletal muscle cells. *Diabetes* 2001; 50: 124-1252

Dickinson RB, Guido S, Tranquillo RT. Biased cell migration of fibroblasts exhibiting contact guidance in oriented collagen gels. *Ann. Biomed. Eng.* 1994; 22: 342-56

Dickinson RB, Tranquillo RT. Optimal estimation of cell movement indices from statistical analysis of cell tracking data *AIChE J.* 1993; Vol 39, No.12

Enserink JM, Price LS, Methi T, Mahic M, Sonnenberg A, Bos JL, Taskèn, K. The cAMP-Epac-Rap1 pathway regulates cell spreading and cell adhesion to laminin-5 through the alpha3beta1 integrin but not the alpha6beta4 integrin. *J Biol Chem.* 2004; 22: 44889-44896

Estellés A, Yokoyama M, Nothias F, Vincent JD, Glowinski J, Vernier P, Chneiweiss H. The major astrocytic phosphoprotein PEA-15 is encoded by two mRNAs conserved on their full length in mouse and human. *J Biol Chem.* 1996; 271(25):14800-6.

Falanga V. Wound healing and its impairment in the diabetic foot. *Lancet.* 2005;366:1736–1743.

Fiory F, Formisano P, Perruolo G, Beguinot F. PED/PEA-15, a multifunctional protein controlling cell survival and glucose metabolism. *Am. J. Physiol. Endocrinol. Metab.* 2009; 297: 592-601

Galiano R.D., et al. Topical vascular endothelial growth factor accelerates diabetic wound healing through increased angiogenesis and by mobilizing and recruiting bone marrow–derived cells. *Am. J. Pathol.* 2004;164:1935–1947.

Galkowska H., Wojewodzka U., Olszewski W.L. Chemokines, cytokines, and growth factors in keratinocytes and dermal endothelial cells in the margin of chronic diabetic foot ulcers. *Wound Repair Regen.* 2006;14:558–565.

Giacco F, Perruolo G, D'Agostino E, Fratellanza G, Perna E, Misso S, Saldalamacchia G, Oriente F, Fiory F, Miele C, Formisano S, Beguinot F, Formisano P. Thrombin-activated platelets induce proliferation of human skin fibroblasts by stimulating autocrine production of insulin-like growth factor-1. *FASEB J.* 2006; 20:2402-4.

Goalstone ML. What does insulin do to RAS? *Cell Signal.* 1998;10:297-301

Gibran N.S., et al. Diminished neuropeptide levels contribute to the impaired cutaneous healing response associated with diabetes mellitus. *J. Surg. Res.* 2002;108:122–128.

Goren I, Muller E, Pfeilschifter J, Frank S. Severely impaired insulin signaling in chronic wounds of diabetic ob/ob mice: a potential role of tumor necrosis factor- $\alpha$ . *Am J Pathol* 2006; 168: 765–77.

Guedez L, Rivera A, Salloum R, Miller M, Diegmüller J, Bungay P, Stetler-Stevenson W. Quantitative Assessment of Angiogenic Responses by the Directed *in Vivo* Angiogenesis Assay. *American Journal of Pathology* 2003; 162: 1431-1439

Hannan D, Folkman J. Patterns and emerging mechanisms of the angiogenic switch during tumorigenesis. *Cell* 1996; 86 (3): 353-364

Harrison - Principi di Medicina Interna - Il Manuale 17/ed March 2009

Hattori N, Mochizuki S, Kishi K, Nakajima T, D'Armiento J, Okada Y. MMP-13 plays a role in keratinocyte migration, angiogenesis, and contraction in mouse skin wound healing. *Am. Journ. of Path.* 2009; 175: 533-546

Horikawa Y, et al. Genetic variation in the gene encoding calpain-10 is associated with type-2 diabetes mellitus. *Nature Genet.* 2000; 26:163-175.

Huang C, Jacobson K, Schaller MD. MAP kinases and cell migration. *J Cell Sci.* 2004; 5: 4619-28. Review.

Hubner G, Griseldi S. Differential regulation of proinflammatory cytokines during wound healing in normal and glucocorticoid-treated mice. *Cytokine* 1996; 8:548

Huvenners S, Danen, EH. Adhesion signaling- crosstalk between integrins, Src and Rho. *J Cell Sci* 2009; 122:1059-1069

Jaken, S. Protein kinase C isozymes and substrates. *Curr Opin Cell Biol.*1996; 8(2):168-173

Kitsberg D, Formstecher E, Fauquet M, Kubes M, Cordier J, Canton B, Pan G, Rolli M, Glowinski J, Chneiweiss H. Knock-out of the neural death effector domain protein PEA-15 demonstrates that its expression protects astrocytes from TNFalpha-induced apoptosis. *J. of Neuro* 1999;19(19):8244–8251

Krueger J, Chou F, Glading A, Schaefer E, Ginsberg M. Phosphorylation of Phosphoprotein Enriched in Astrocytes (PEA-15) Regulates Extracellular Signal-regulated Kinase-dependent Transcription and Cell Proliferation. *Molecular Biology of the Cell* 2005; 16: 3552–3561

Lawrence WT. Physiology of the acute wound. *Clin Past Surg* 1998; 25:321-40

Lerman OZ, Galiano D, Armour M, Levine JP, Guter CG. Cellular Dysfunction in the Diabetic Fibroblast Impairment in Migration, Vascular Endothelial Growth Factor Production, and Response to Hypoxia. *American Journal of Pathology* 2003; 162: 303-312

Lincoln D, Larsen A, Phillips P, Bove K. Isolation of murine aortic endothelial cells in culture and the effects of sex steroids on their growth. *Cell. Dev. Biol.* 2003; 39:140-145

Liu R, Bal HS, Desta T, Behl Y, Graves DT. Tumor necrosis factor-alpha mediates diabetes-enhanced apoptosis of matrix-producing cells and impairs diabetic healing. *Am J Pathol* 2006; 168:757–64.

Lobmann R., et al. Expression of matrix-metalloproteinases and their inhibitors in the wounds of diabetic and non-diabetic patients. *Diabetologia.* 2002;45:1011–1016.

Maruyama K., et al. Decreased macrophage number and activation lead to reduced lymphatic vessel formation and contribute to impaired diabetic wound healing. *Am. J. Pathol.* 2007;170:1178–1191.

Matthes T, Gruler H. Analysis of cell locomotion. Contact guidance of human polymorphonuclear leukocytes. *Eur. Biophys. J.* 1998; 15: 343-57

Miele C, Raciti GA, Cassese A, Romano C, Giacco F, Oriente F., Paturzo F, Andreozzi F, Zabatta A, Troncone G, Bosch F, Pujol A, Chneiweiss H, Formisano

P, Beguinot F. PED/PEA-15 regulates glucose-induced insulin secretion by restraining potassium channel expression in pancreatic beta-cells. *Diabetes* 2007; 56(3): 622-33

O'Brien BA, Geng X, Orteu CH, Huang Y, Ghoreishi M, Zhang Y, Bush JA, Li G, Finegood T, Dutz JP. A deficiency in the in vivo clearance of apoptotic cells is a feature of the NOD mouse. *J autoimmune* 2006; 26:104–15.

Raftopoulou, M., and Hall, A. Cell migration: Rho GTPase lead the way *Dev. Biol.* 2004; 265: 23-32

Ramos JW, Hughes PE, Renshaw MW, Schwartz MA, Formstecher E, Chneiweiss H, Ginsberg MH. Death effector domain protein PEA-15 potentiates Ras activation of extracellular signal receptor-activated kinase by an adhesion-independent mechanism. *Biol. of Cell* 2000; 11:2863-2872

Ridley A J, Schwartz MA, Burridge K, Firtel RA, Ginsberg MH, Borisy G, Parsons JT, Horwitz AR. Cell migration: integrating signals from front to back. *Science* 2003; 302:1704-9.

Senger DR, Ledbetter SR, Claffey KP, et al. Stimulation of endothelial cell migration by vascular permeability factor/vascular endothelial growth factor through cooperative mechanisms involving the  $\alpha$ v $\beta$ 3 integrin, osteopontin, and thrombin. *Am J Pathol* 1996;149:293–305.

Schlessinger J. How receptor tyrosine kinase activate RAS. *Trends Biochem Sci* 1993;18(8):273-5

Schmeichel AM, Schmelzer JD, Low PA. Oxidative injury and apoptosis of dorsal root ganglion neurons in chronic and experimental diabetic neuropathy. *Diabetes* 2003; 52: 165-171

Schonfelder U, Abel M, Wiegand C, Klemm D, Elsner P, Hipler UC. Influence of selected wound dressings on PMN elastase in chronic wound fluid and their antioxidative potential in vitro. *Biomaterials* 2005; 26:6664–673.

Schulze WX, Deng L, Mann M. Phosphotyrosine interactome of the ErbB-receptor kinase family. *Molecular systems biology* 2005; 1.

Schultz GS, Wysocki A. Interactions between extracellular matrix and growth factors in wound healing. *Wound Repair Regen.* 2009; 17:153-62.

Sibbald RG, Woo K, Ayello EA: Increased bacterial burden and infection: the story of NERDS and STONES. *Adv Skin Wound Care* 2006; 19:447-461.

Sibbald RG, Woo K. The biology of chronic foot ulcers in person with diabetes. *Diabetes Metab Res Rev* 2008; 24: 25-30

Takamiya M, Fujita S, Saigusa K, Aoki Y. Simultaneous detection of eight cytokines in human dermal wounds with a multiplex bead-based immunoassay for wound age estimation. *Int J Legal Med* 2008; 122: 143–148.

Trousdale RK, Jacobs S, Simhae D A, Wu J K, Lustbader JW. J. Wound Closure and metabolic parameter variability in db/db mouse model for diabetic ulcers. *Surg. Res.* 2009; 151: 100-7

Valentino R, Lupoli GA, Raciti GA, Oriente F, Farinaro E, Della Valle E, Salomone M, Riccardi G, Vaccaro O, Donnarumma G, Sesti G, Hribal ML, Cardellini M, Miele C, Formisano P, Beguinot F. The PEA15 gene is overexpressed and related to insulin resistance in healthy first-degree relatives of patients with type 2 diabetes. *Diabetologia.* 2006; 49(12):3058-66.

Velander P, Theopold C, Hirsch T, Bleiziffer O, Zuhaili B, Fossum M, Hoeller D, Gheerardyn R, Chen M, Visovatti S, Svensson H, Yao F, Eriksson E. Impaired wound healing in an acute diabetic pig model and the effects of local Hyperglycemia. *Wound Repair Regen.* 2008; 16: 288-93

Vial E, Sahai E, Marshall CJ. ERK-MAPK signaling coordinately regulates activity of Rac1 and RhoA for tumor cell motility. *Cancer cell* 2003; 4:67-79

Vigliotta G, Miele C, Santopietro S, Portella G, Perfetti A, Maitan MA, Casses eA, Oriente F, Trencia A, Fiory F, Romano C, Tiveron C, Tatangelo L, Troncone G, Formisano P, Beguinot F. Overexpression of the ped/pea-15 gene causes diabetes by impairing glucose-stimulated insulin secretion in addition to insulin action. *Mol Cell Biol.* 2004; 24(11):5005-15.

Villeneuve LM, Natarajan R. The role of epigenetics in the pathology of diabetic complications. *Am J Physiol Renal Physiol.* 2010;299(1):14-25.

Wall IB, Moseley R, Baird DM, Kipling D, Giles P, Laffafian I, Price PE, Thomas DW, Stephens PJ. Fibroblast dysfunction is a key factor in the non-healing of chronic venous leg ulcers. *Invest. Dermatol.* 2008; 128:2526-40.

Wang X, Chen S, Jin H, Hu R. Differential analyses of angiogenesis and expression of growth factors in micro- and macrovascular endothelial cells of type 2 diabetic rats. *Life Sciences* 2009; 84:240–249

Weinstein D, Kirsner R. Refractory ulcers: role of tumor necrosis factor- $\alpha$ . *J Am Acad Dermatol* 2010;63:146-54.

Werner S, Grose R. Regulation of wound healing by growth factors and cytokines. *Physiol Rev* 2003; 83: 835-70

Wetzler C, Kampfer H, Stallmeyer B, Pfeilschifter J, Frank S. Large and sustained induction of chemokines during impaired wound healing in the genetically diabetic mouse: prolonged persistence of neutrophils and macrophages during the late phase of repair. *J Invest Dermatol* 2000; 115:245–53.

Witt D, Lander AD. Differential binding of chemokines to glycosaminoglycan subpopulations. *Curr Biol* 1994;4:394–400.

Woo K, Ayello EA, Sibbald RG. The edge effect: current therapeutic options to advance the wound edge. *Adv Skin Wound Care*. 2007; 20: 99-117.

Zarich N, Oliva JL, Martinez N, Jorge R, Ballester A, Gutierrez-Eisman S, Garcia-Vargas S, Rojas JN. Grb2 Is a Negative Modulator of the Intrinsic Ras-GEF Activity of hSos1. *Molecular Biology of the Cell* 2006; 17(8): 3591-7